Nano Research

ISSN 1998-0124 CN 11-5974/O4
https://doi.org/10.1007/s12274-021-3388-x

Review Article

Functional photonic structures for external interaction with flexible/wearable devices

Young Jin Yoo[1,§], Se-Yeon Heo[1,§], Yeong Jae Kim[2,§], Joo Hwan Ko[1], Zafrin Ferdous Mira[1], and Young Min Song[1,3,4] (✉)

[1] *School of Electrical Engineering and Computer Science, Gwangju Institute of Science and Technology (GIST), 123 Cheomdangwagi-ro, Bukgu, Gwangju 61005, Republic of Korea*
[2] *Korea Institute of Ceramic Engineering & Technology, Ceramics Test-Bed Center, 3321 Gyeongchung-daero, Sindun-myeon, Icheon-si Gyeonggi-do 17303, Republic of Korea*
[3] *Anti-Viral Research Center, Gwangju Institute of Science and Technology (GIST), 123 Cheomdangwagi-ro, Bukgu, Gwangju 61005, Republic of Korea*
[4] *AI Graduate School, Gwangju Institute of Science and Technology (GIST), 123 Cheomdangwagi-ro, Bukgu, Gwangju 61005, Republic of Korea*
[§] *Young Jin Yoo, Se-Yeon Heo, and Yeong Jae Kim contributed equally to this work.*

Received: 1 December 2020 / **Revised:** 15 January 2021 / **Accepted:** 5 February 2021

ABSTRACT

In addition to vital functions, more subsidiary functions are being expected from wearable devices. The wearable technology thus far has achieved the ability to maintain homeostasis by continuously monitoring physiological signals. The quality of life improves if, through further developments of wearable devices to detect, announce, and even control unperceptive or noxious signals from the environment. Soft materials based on photonic engineering can fulfil the abovementioned functions. Due to the flexibility and zero-power operation of such materials, they can be applied to conventional wearables without affecting existing functions. The achievements to freely tailoring a broad range of electromagnetic waves have encouraged the development of wearable systems for independent recognition/manipulation of light, pollution, chemicals, viruses and heat. Herein, the role that photonic engineering on a flexible platform plays in detecting or reacting to environmental changes is reviewed in terms of material selection, structural design, and regulation mechanisms from the ultraviolet to infrared spectral regions. Moreover, issues emerging with the evolution of the wearable technology, such as Joule heating, battery durability, and user privacy, and the potential solution strategies are discussed. This article provides a systematic review of current progress in wearable devices based on photonic structures as well as an overview of possible ubiquitous advances and their applications, providing diachronic perspectives and future outlook on the rapidly growing research field of wearable technology.

KEYWORDS

photonic structure, wearable device, health care device, colorimetric sensor, radiative cooling, infrared camouflage

1 Introduction

Multifunctional wearable systems on human skin are capable of detecting subtle physiological changes that occur gradually in daily life through real-time monitoring, thus facilitating drug delivery and/or implementation of appropriate therapies based on the diagnosis of the corresponding symptoms [1–4]. This integrated care helps maintain homeostasis, which is an essential element of life support through rapid treatment of acute symptoms and continuous management of chronic diseases. Furthermore, functional materials such as dynamic gels and biopolymers show unprecedented potential for smart skins with a variety of tunable properties including mechanical strength, toughness, viscoelasticity, self-healing, and ionic conductivity [5–7]. Despite the efficient capabilities of existing wearable technologies, these skin-interfaced devices, embedded under a flexible patch, mainly facilitate monitoring of internal signals from human beings. A wearable device can obtain information such as glucose levels, temperature, blood pressure, and oxygen saturation via vital signs (i.e., respiration rate and electrocardiography) [8–15]. However, the detection of rapid environmental changes, such as abnormal weather and pandemic pathogens, exceeds the range of human physiological adaptation and, thus, can be realized by external monitoring. Furthermore, by supplementing the lopsided build and function of existing wearable devices, external and internal signal management solutions that quickly detect external stimuli and enable preemptive internal actions must be provided.

Recent advances in photonic structures and materials have opened up the possibility of detecting and managing external environmental stimuli such as light, pollutants, chemicals, viruses, and heat, even on flexible substrates [16–30]. These photonic structures are used for optical sensing over ultraviolet (UV) to visible (Vis) spectral regions, and for wearable heat control and ubiquitous applications in the mid- to far-infrared (IR) spectral regions. In this regard, several types of photonic structures are introduced on flexible substrates for integration and use in wearables. For instance, in colorimetric sensing, visible signals (280–800 nm) are detected, indicating changes in the external environment, enabling intuitive detection in

Address correspondence to ymsong@gist.ac.kr

real time without additional processing and analysis [31–38]. The applications include chemical and virus detection for the intuitive protection of wearable device users [24, 39–44]. The radiative cooling strategy, which independently operates across solar (280–2,500 nm) and far-IR spectral ranges (8–13 μm), addresses device heating and battery power issues [45–49]. Recent achievements in mid- and far-IR plasmonic engineering (2–20 μm) have also contributed significantly to the security and safety of next-generation devices offering undercover operation and IR sensing [50–53].

This review discusses state-of-the-art technology for detecting/managing external environmental stimuli using flexible photonic structures and materials and highlights the convergence of these optical/thermal schemes with flexible wearable devices. Section 2 presents the concept of total internal/external care with external environmental stimuli. Sections 3–5 introduce photonic structures and multifunctional applications on flexible substrates and wearable devices, recently reported radiative cooling structures, and recent ubiquitous techniques on flexible substrates. This review ends with a strategy for the development of a fully integrated multifunctional internal/external care wearable system with future directions and opportunities for external environmental stimulus detection for flexible/wearable devices.

2 External photonic structures for surrounding monitoring/management

The human body must detect and respond to changes in its internal and external environments, because human body conditioning needs to be carefully controlled for it to function effectively and survive. Human organs and tissues react sensitively to external stimuli and sometimes suffer minor or severe damage. For example, environmental factors such as temperature and noise level can change the heart rate. Acid rain and pollution from industrialized areas are typically associated with a high incidence of infections and respiratory diseases such as chronic lung disease. Beyond the self-action of the human body, proactive internal care through external sensing and management is likely to become a primary prevention mechanism against human disease.

Figure 1 provides a broad overview of external/internal care configured with external photonic structures for the detection and management of external environmental stimuli. In recent decades, wearable devices for internal healthcare have been actively studied, and several researchers have highlighted wearable devices having specific functions [15, 54–58]. Early advances in epidermal wearable sensing platforms focused on single analyte detection using a wide range of target analytes [59–63]. These devices were made using stress-resistant materials and sensor structures to achieve a high degree of skin conformability, which is essential for reliable sweat sampling during exercise, such as in tattoo-type platforms [64–68]. Recent advances in flexible hybrid electronics and microfluidics have resulted in a new class of physiological and biochemical sensors that non-invasively capture and investigate biofluids such as sweat, tears, and saliva [14, 54, 69–71]. In particular, the state of the art in wearable colorimetric and electrochemical sweat detection technology emphasizes the convergence of these detection modalities and epidermal electronic and physiological monitoring [55, 69, 72, 73]. The proposed hybrid biochemical/physiological monitoring system opens a wide range of possibilities for a fully integrated multimode physical biochemical wearable system [4, 74].

In conventional clinics, numerous light-based diagnostic and treatment devices are routinely used. These devices have a familiar format, such as an object that is mounted on a wall or

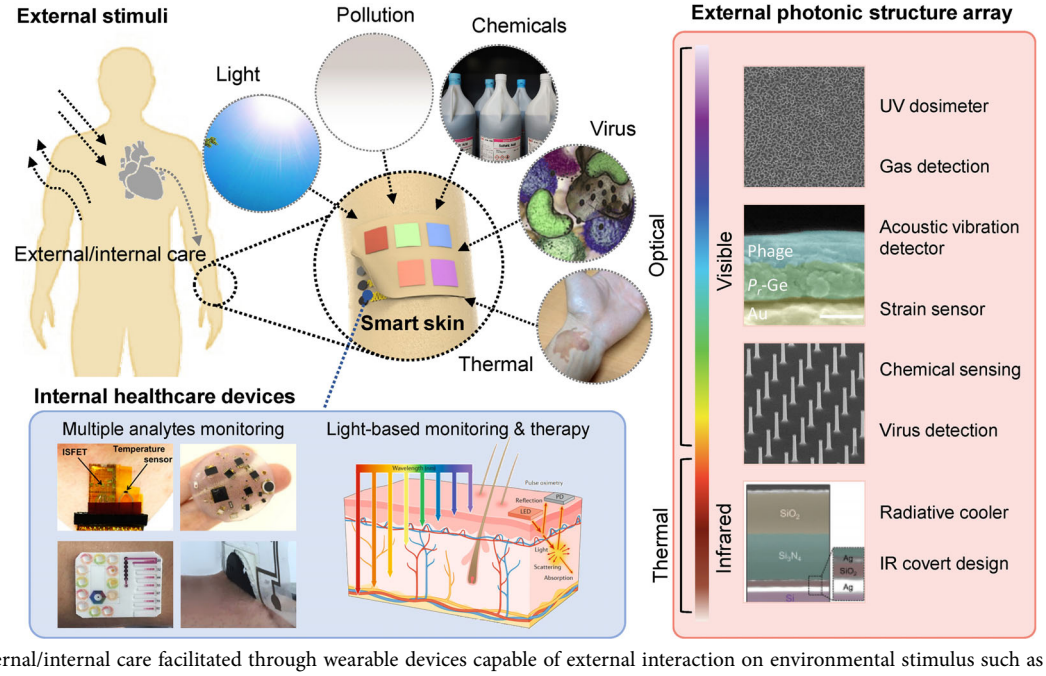

Figure 1 External/internal care facilitated through wearable devices capable of external interaction on environmental stimulus such as light, pollution, chemicals, thermal and virus, etc. (left-top) External interactions on the wearable device enable adaptive healthcare by fusion with recently advanced internal devices such as multiple analytes monitoring and light-based monitoring and therapy (left-bottom). Reproduced with permission from Ref. [74], © American Chemical Society 2017; Ref. [17], © Jang, K.-I. et al. 2017; Ref. [19], © American Chemical Society 2019; Ref. [21], © WILEY-VCH Verlag GmbH & Co. KGaA, Weinheim 2017; and Ref. [57], © Springer Nature Limited 2020, respectively. Light-based photonic structures classified into two optical and thermal regions (right): 1) optical sensing in UV and real-time human eye detection in visible region, ultraviolet dosimeter, gas detection, and colorimetric sensing detection of chemicals, virus, temperature, etc.; and 2) thermoregulation in the far-IR region, radiative cooler and IR covert designs. Reproduced with permission from Ref. [16], © WILEY-VCH Verlag GmbH & Co. KGaA, Weinheim 2016; Ref. [98], © WILEY-VCH Verlag GmbH & Co. KGaA, Weinheim 2020; Ref. [97], © American Chemical Society 2019; and Ref. [129], © WILEY-VCH Verlag GmbH & Co. KGaA, Weinheim 2018, respectively.

placed next to a patient's bed. However, many new ideas have recently been proposed for the realization of implantable or wearable functional devices [75–77]. Many advances have been made with the development of multifunctional materials for photonic healthcare devices [57]. For typical healthcare monitoring, photonic diagnosis through pulse oximetry uses light-emitting diodes and photodetectors (PDs) to detect light absorption in peripheral blood [78]. Representative phototherapeutic methods include photothermal therapy, where photo-induced thermal ablation is used on diseased tissues, and photodynamic therapy, which uses reactive oxygen species (ROS) produced by photosensitizers [79, 80]. In addition, photobiomodulation uses light stimulation of mitochondrial chromophores to produce nitric oxide (NO), ROS, and adenosine triphosphate (ATP) [81].

Highly developed internal healthcare devices with functions such as monitoring, drug delivery, and therapy can be integrated for preemptive care in conjunction with external sensing. External/internal care systems can be used in several flexible/wearable forms such as scopolamine and transdermal patches, which can be directly attached to the affected human body or organs for disease/drug monitoring and therapy without interfering with a person's daily activities. Around us, external environmental factors such as light, pollution, chemicals, viruses, and heat that may have minor or major effects on the human body must be continuously detected and managed. From this point of view, we highlight an overview of the state-of-the-art photonic applications for external detection and management of the external environmental factors on flexible/wearable devices. Multifunctional photonic structures provide vast information using signals that range from UV to far-IR region for protection against external stimuli. The following content highlights the most advanced preliminary health status/diagnosis systems, which comprise light-based photonic structures classified into two electromagnetic wave regions: 1) real-time human eye detection in the visible region (colorimetric sensing of chemicals, viruses, temperature, etc.) and 2) thermoregulation in the mid- and far-IR regions (radiative cooler, IR encoding/decoding).

3 Photonic structures for external monitoring in UV–Vis–NIR range

In nature, photonic structures have been observed in living organisms that have evolved over millions of years to create a colorful natural world. In particular, the photonic features observed in certain natural organisms, such as butterflies and beetles, produce brilliant colors depending on the surrounding environment [82, 83]. These concomitant colors are caused by visible light interference due to micro/nanoscale structures that are optically affected by the external environment [84]. Radical threats, including hazardous substances from industrialization and infectious diseases spreading worldwide, are overwhelming human adaptability and/or immunity, further emphasizing the need for external monitoring. Inspired by nature, the surrounding dependency of the structural coloring scheme provides possibilities for visual monitoring of various external environmental stimuli.

Typically, photonic crystals are highly ordered structures with lattice parameters in the wavelength range of the propagating light. Their optical and geometrical properties lead to the formation of a photonic energy band structure, which can allow or inhibit the propagation of electromagnetic waves in a limited frequency range. These unique properties have attracted much interest in the study of artificial photonic structures for structural color applications [85]. The combination of design methods for typical sophisticated photonic crystal structures relies on highly ordered structures and/or periodically ordered structures. Therefore, complex structural or material modifications are required to deal with various external changes that affect key optical properties such as refractive index and thickness [86]. Moreover, the complex assembly of precisely aligned nano/microstructures and diverse materials to achieve optically high sensitivity limits the uniform color and stable response of various shapes/surfaces [87].

Recent advances in nanofabrication and ingenious approaches to structural color have opened up possibilities of photonic structures for sensitive color change in response to external environmental stimuli in diverse shapes/surfaces. In this section, we summarize the different types of photonic structures applicable to flexible substrates and wearable devices. We classify photonic structures according to the color development mechanisms of additive and subtractive colors and review their optical and chromaticity properties. For external monitoring applications, we compare the performances of representative photonic-structure-based colorimetric sensors, and introduce various photonic structures for multifunctional detection.

3.1 Spectrally responsive photonic structures on flexible substrates

Over the past decade, numerous materials have been developed for wearable devices with properties such as deformability, flexibility, and stretchability. Flexible materials enable the convergence of applications by providing a substrate for an integrated system of various sensors or structures whose applications were limited with conventional rigid substrates. In this section, the various types of photonic structures implemented on materials that enable the flexibility of wearable devices are discussed, as shown in Fig. 2(a). In particular, the structural color characteristics of photonic structures, including multilayers, inverse opal structures, ultrathin layers, and micro/nano-arrays, on flexible substrates according to different coloring mechanisms are described in detail.

The coloring mechanism consists of two main types: additive and subtractive colors. The additive color mechanism creates a new color by adding one set of wavelengths to another. Additive color mixing occurs when light of different wavelengths is mixed. In additive colors, the primary colors are red, green, and blue (RGB), forming an area of RGB gamut in the CIE color coordinate system (CIE 1931 standard observer). Typically, the structural color by the transmission/reflection peaks in the visible spectrum follows the additive color mechanism (Fig. 2(b)). In contrast, the subtractive color mechanism creates a new color by the removal of wavelengths from light with a broad wavelength spectrum. Subtractive color mixing occurs when we mix paints, dyes, or pigments. In subtractive colors, the primary colors are cyan, magenta, and yellow (CMY), forming an area of CMY gamut in the CIE color coordinate system. Conventionally, the structural color by the transmission/reflection dips in the visible spectrum follows the subtractive coloring mechanism (Fig. 2(c)).

3.1.1 *Additive coloring structures*

To generate clear coloration using additive color mixing, numerous flexible light interference methods have been introduced, such as multi-stacking structural [88], inverse opal structures [85, 89], and nanostructure array [90]. For example, Chung et al. inspired by Morpho butterfly wings, stacked eight pairs of TiO_2 and SiO_2 layers, resulting in clear and flexible coloration with reflectance peaks (Fig. 2(d)).

In other words, using regularly arranged optical structures, electromagnetic waves can be strongly modulated by manipulating

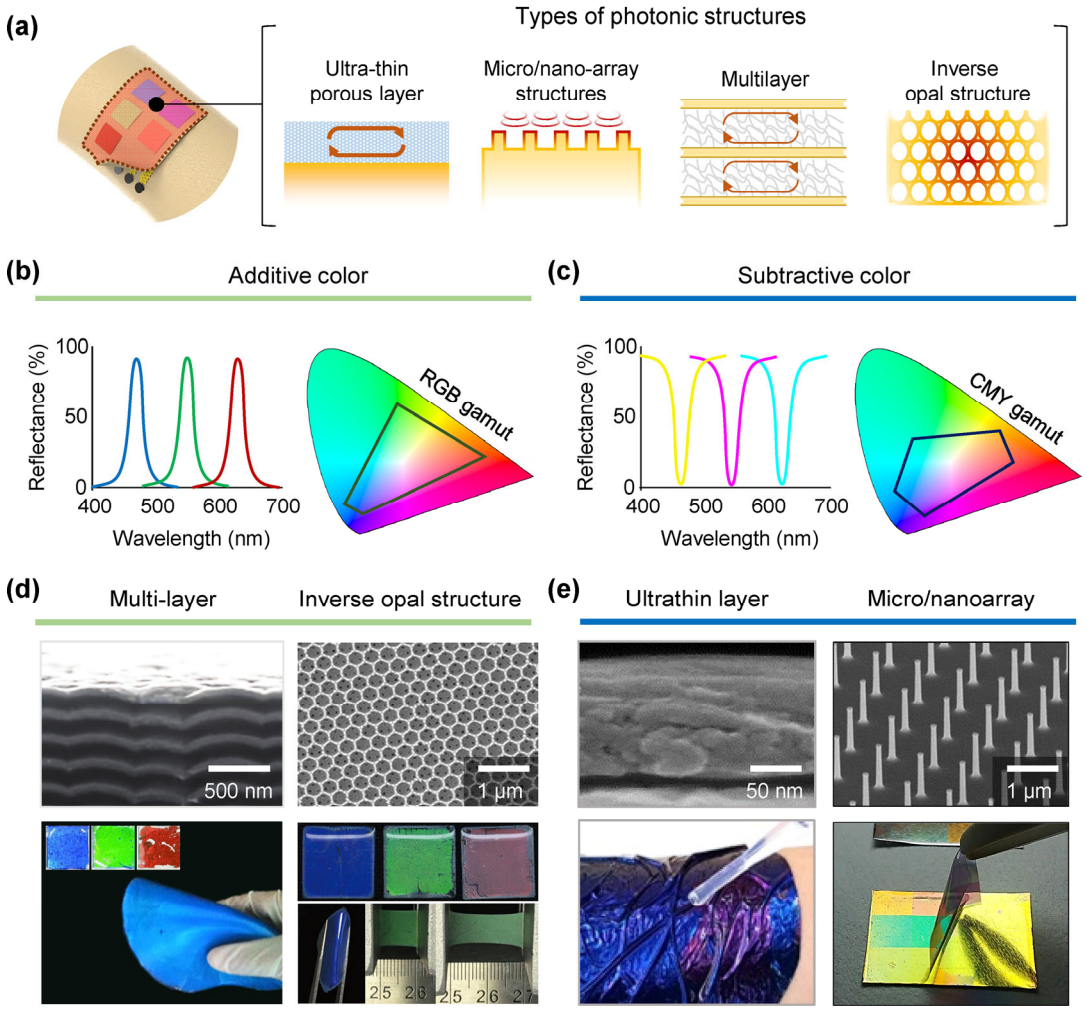

Figure 2 (a) Various types of photonic structures with the flexibility of wearable devices. (b) Additive and (c) Subtractive structural coloration. (d) Morpho-butterfly-inspired structure (left). Reproduced with permission from Ref. [88], © WILEY-VCH Verlag GmbH & Co. KGaA, Weinheim 2012. Inverse opal structure (right). Reproduced with permission from Ref. [85], © American Chemical Society 2018. (e) Ultrathin film layer (left). Reproduced with permission from Ref. [96], © American Chemical Society 2020. Polymer-embedded vertical nanowire arrays (right). Reproduced with permission from Ref. [97], © American Chemical Society 2019.

the propagation of photons using the photonic band gap (PBG). For example, Liu et al. placed a periodical arrangement of the inverse opal structure. By modulating the PBG, the reflected color shows tunability with non-iridescent (angle-insensitive) structural color properties (Fig. 2(d)). Interestingly, using this color tunability of PBG materials, Fu et al. inspired by chameleons showed a dynamically changeable photonic crystal by modifying the period of the structure for sensing strain [89]. Over the spectral range, UV light with wavelength ranging from 10 to 400 nm should be considered because of its ability to damage DNA or cause skin cancer. Following these needs for management, the UV light detection technology has been developed [91–93]. Using the property that UV light cross-links silk, Wang et al. irradiated UV light into a silk inverse opal to gradually compress the lattice [93]. Consequently, the central wavelength of the stop-band decreased linearly with the blueshift behavior.

3.1.2 Subtractive coloring structures

In the case of subtractive color, several strategies for strong resonance and selective absorption have been developed, including coating with highly absorbing material, periodic arrangement, and multilayer stacking [94–96]. Kats et al. introduced an ultrathin coating layer for the strong selective absorption of light [94]. In this work, highly absorbing dielectrics were applied as a coating layer onto a metal substrate, which acted as a strong absorber that rapidly attenuated the incident light. Using this simple concept, Yoo et al. showed an ultrathin and flexible colorimetric sensor platform by depositing an absorbing material onto a flexible and thin substrate (Fig. 3(e)) [95. 96]. To sensitively absorb visible light for higher saturation of coloration, periodic micro arrays of nanostructures can support the enhancement of color purity. As shown in Fig. 3(e), the arranged nanowires have a role in selective light absorption for enhancing color purity [97].

3.2 Externally modulated structures with functional materials

For practical external monitoring, photonic structures can allow for a wide-scale colorimetric detection with functional materials. Colorimetric detection, which converts environmental changes into visible color changes, is a simple yet effective detection technique suitable for the development of low-cost and low-power sensors. An effective approach to colorimetric detection utilizes the structural color of photonic structures to create environmentally affected color-changeable materials. In this section, photonic structures for broad-scale external monitoring of flexible substrates are introduced. We discuss several functional photonic structures with detailed comparison of

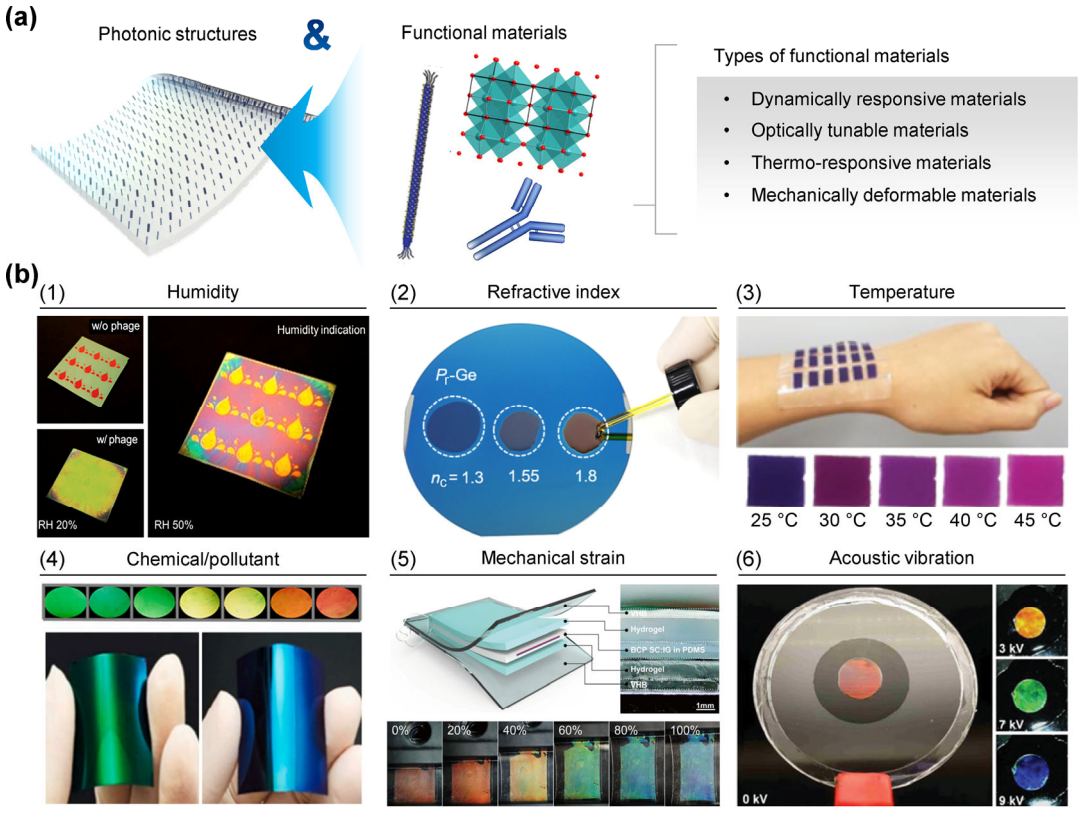

Figure 3 (a) Structural color combined with functional materials (e.g., dynamically responsive materials, optically tunable materials, thermo-responsive materials, mechanically deformable materials) for colorimetric sensing. (b) (1) Humidity sensor using phage materials. Reproduced with permission from Ref. [98], © WILEY-VCH Verlag GmbH & Co. KGaA, Weinheim 2020. (2) Refractive index senor using highly lossy porous medium. Reproduced with permission. Reproduced with permission from Ref. [96], © American Chemical Society 2020. (3) Temperature sensing by thermal color indicator. Reproduced with permission from Ref. [27], © Choe, A. et al. 2018. (4) Chemical/pollutant sensing using polymer multilayer. Reproduced with permission from Ref. [100], © Elsevier B.V. 2020. (5) Mechanical strain sensor using hydrogel. Reproduced with permission from Ref. [107], © American Chemical Society 2018. (6) Acoustic vibration sensor. Reproduced with permission from Ref. [108], © WILEY-VCH Verlag GmbH & Co. KGaA, Weinheim 2019.

their colorimetric detection performance.

3.2.1 *Dynamically responsive materials*

To detect humid atmospheric environments, several approaches have been suggested, including nanofibrous virus materials [98], hydrogels [34], and multi-layered organic materials [99]. Basically, sensing the external environment via color change requires a dynamic layer that contributes to structural color generation. For example, Yoo et al. introduced an M13 bacteriophage of fibrous virus that expands with increasing humidity as a sensing layer [98]. To detect this expansion as a color change, a resonating layer was used. Furthermore, the ultrathin scale of the virus layer enabled high-speed sensing. Finally, as depicted in Fig. 3(b), the patterned humidity sensor shows a dynamic response corresponding to humidity change. For practical applications including the detection of chemicals and pollutants, virus-coated ultrathin colorimetric sensors have been successfully tested on the parts-per-billion scale for detecting volatile organic compounds (VOCs) and endocrine disrupting chemicals (EDCs). Moreover, as a strategic approach for humidity and chemical detection, hydrogel and polymer multilayers have been designed for fast detection of relative humidity and chemical gas [34, 99]. As a successful demonstration, Jung et al. used a recyclable, chromophore-free flexible multilayer for the sub-parts-per-million-scale vapor-phase colorimetric detection of diethyl chlorophosphate (DCP), a nerve agent mimic, with humidity control sensitivity [100]. In addition, as a co-assembly approach proposed by Bai et al., owing to its high flexibility due to the plasticizing effect, a cellulose nanocrystal film could detect various external stimuli including compression and contents of ethanol and alkali through color change [101]. The resonance/interference condition of the suggested structure was changed by the expansion/shrinkage of the organic layer, resulting in humidity sensing through dynamic color change. As another strategy, Gallego-Gómez et al. presented an artificial three-dimensional opal structure for detection humidity. Due to the vaporized water, the opal spaces were gradually filled and this increased the average refractive index, leading to a change in the photonic bandgap [102].

3.2.2 *Optically tunable materials*

For more universal detection, multifunctional photonic structures have been introduced, such as thin-film resonators [96], inverse opal structures [103], and nano-hole arrays [86]. Generally, the sensing of refractive index is based on the change of the phase shift and interference condition. For example, Yoo et al. developed a simple and tunable refractive index sensor with a thin-film resonator [96]. By applying the absorbing layer onto the metal layer, the phase shift of the reflected light is amplified, resulting in a sensitive change in the resonating condition. Because the resonance condition can be easily controlled over the visible wavelength range, the changed resonating condition manifested as a visible color response. For a more drastic color change, several structures have been suggested, including periodic nanostructures (inverse opal and nano-hole array). Kim et al. introduced an inverse opal structure based on the silk material and showed the color change by changing the bandgap frequency [103]. Because the distance or index contrast change induces a bandgap frequency

change, the dimension of the inverse opal structure determines the refractive index sensing condition.

3.2.3 *Thermoresponsive materials*

As another type of multifunctional colorimetric sensors, several thermoresponsive colorimetric sensors have been developed by controlling the optical resonance condition corresponding to temperature change. To control the thermoresponsive reaction under thermal stimuli, poly (nisopropylacrylamide) (PNIPAM) [27], quantum dots (QDs) [104], and carbon dots (CDs) [105] have been used to manipulate resonating conditions. For example, Choe et al. showed a color shift between red and grayish violet with a peak shift of 176 nm based on reversibly swollen and shrunken behavior [27]. The physically dynamic change induced a plasmonic resonance condition change resulting in a gradual shift of color. Furthermore, the modulating fluorescent condition of QDs has also been introduced. Jiang et al. showed a thermoresponsive property by mixing blue fluorescent polyurethane (PU) and green-yellow fluorescent CDs [104]. By adjusting the ratio of CDs to PU, the fluorescence of the PU/CD composite decreased, whereas the blue component did not change. Furthermore, Zhang et al. developed a dual-emitting fluorescent phosphor by grafting $SrAl_2O_4$, Eu^{2+}, Dy^{3+} onto CDs using a core shell process; this phosphor showed a color change due to thermal stimuli from 243 to 383 K [106]. Detailed comparison of specification, structure, and material information for humidity, refractive index, temperature, and chemical sensors is shown in Table 1.

3.2.4 *Mechanically deformable materials*

Additionally, based on the principle of colorimetric sensing through modulated resonating/interference conditions, there are also many other functional and useful applications [87, 107, 108]. For example, based on the conversion of a metal to its hydride, which induces mechanical expansion, hydrogen gas sensors have been fabricated. Duan et al. demonstrated a hydrogen sensor based on magnesium (Mg), which can react with hydrogen molecules to produce metallic hydride (i.e., MgH_2) [87]. Because the volume expansion of Mg induces a change in the plasmonic condition, the plasmonic display changes color. As can be seen in the example above, the mechanical change causes the resonance condition to change. Park et al. showed a strain-sensitive structural color sensor [107]. By combining the mechanochromic bilayer of ionic gel, based on the presence of an ionic liquid as a block copolymer domain with a one-dimensional (1D) periodic lamella, the mechanical strain was directly visualized. With a strategic design of the optical resonating layer, interesting and useful colorimetric sensing applications have been reported. For instance, Kim et al. demonstrated a colorimetric acoustic vibration sensor using close-packed polystyrene (PS) beads. To induce sufficient color change of the PS bead structure, a stretchable substrate is introduced, which shows the areal strain by direct current (DC) bias. Using this platform, corresponding to the frequency of the acoustic wave, the reflected color showed a drastic color change [108].

4 IR management

Driven by the desire to advance our understanding of human physiology, wearable devices have been applied for various purposes, including miniaturization, optimization of battery power and working lifetime, and enhancement of biocompatibility. However, the portable technology faces the inevitable problem of Joule heating as the heat generation of the devices increases with increasing integration density [111]. It limits the performance and reliability of mobile devices, as heat induces energy consumption, aging, and failure in user comfort [112]. In addition, in a wearable device that is in close contact with the skin, the accumulated heat leads to inaccurate signal acquisition from the body. Accordingly, there is a critical need to develop effective thermal management strategies, especially for small-sized devices.

Thermal energy is characterized by the Stefan–Boltzmann law, $P = \varepsilon\sigma T^4$, where ε is the emissivity of the object, σ is the Stefan–Boltzmann constant, and T is the temperature of the surface. All objects with a surface temperature above absolute zero (−273.15 °C) emit electromagnetic radiation, which is proportional to their intrinsic temperature [113]. When the temperature of the object is fixed at ambient temperature (~ 22 °C), the thermal radiation energy primarily arises from the IR wavelength of 8–25 μm [114]. Therefore, one can engineer the heat dissipation of the device by regulating the IR radiation of the materials.

Furthermore, IR-spectrum engineering is accompanied by the ubiquitous modern technology of IR stealth [115, 116], anti-counterfeiting [117, 118], detection [119, 120], and optical holography [113, 121]. The advent of thermally imperceptible property promises to satisfy security and confidentiality, which has attracted increasing attention for many commercial and surveillance applications [114, 117, 122–124]. Owing to the scalability of Maxwell's equation, microstructure engineering can be extended to other electromagnetic spectra from visible to microwave regimes. This inspired many scientists to develop structural-engineering-based devices for thermal camouflage, which is expected to contribute to the development of

Table 1 Photonic structure based colorimetric sensor

Structure	Material	Type	Color model	Wavelength range (nm)	Sensitivity	Reference
Multilayer	TiO_2/P(AM-MBA)	Humidity	Additive	426–668	~ 500 ms	[99]
Tri-layer	M13 Phage/Ge/Au	Humidity	Subtractive	475–625	~ 110 ms	[98]
Opal	SiO_2	Humidity	Additive	475–625	~ 60 ms	[102]
Inverse opal	Silk	Refractive index	Additive	550–700	430 nm/RIU	[103]
Thin-film	Ge/Au	Refractive index	Subtractive	513–600	—	[96]
Nanotemplate	Au/AAO	Refractive index	Subtractive	500–625	348 nm/RIU	[86]
Nanosphere	SiO_2	Temperature	Additive	500–631	15.7–30.2 °C	[109]
Nanoparticle	Au/PNIPAM/PAAm	Temperature	Subtractive	545–721	24–45 °C	[27]
Multilayer	PpMs/PNIPAM	Temperature	Additive	410–710	23–49 °C	[110]
Tri-layer	M13 Phage/Ge/Au	Chemical/pollutant	Subtractive	475–625	10 ppb (VOCs, EDCs)	[98]
Nanoparticle	Cellulose	Chemical/pollutant	Additive	345–601	0.1 g/L (ethanol)	[101]
Multilayer	P(VC-co-BPA)	Chemical/pollutant	Additive	540–630	4 ppm (DCP)	[100]

next-generation soft covert wearables. Here, we summarize the state of the art on IR management for thermoregulation and IR encoding/decoding with regard to portable device applications.

4.1 Passive radiative cooling

Passive radiative cooling is effective as it can address issues related to not only device heating but also battery power. This strategy involves the tailoring of the electromagnetic spectrum in the solar (300–2,500 nm) and far-IR spectral ranges (8–13 μm) to minimize heat gain and maximize outgoing thermal radiation, thus enabling cooling without energy consumption [125–128]. Radiative cooling has an immemorial history; the Saharan silver ants can withstand the hottest terrestrial environments on Earth by effectively resisting overheating from the sun and their own IR radiation [3]. The bodies of the ants are covered by dense arrays of triangular hair that enhance solar reflectivity and increase IR emissivity. The photonic structure and underlying physical mechanisms have provided an abundant source of inspiration for the design of novel optical structures. These include multilayer thin-film structures, microtextured surfaces, porous polymers, and microparticles embedded in flexible substrates, as shown in Fig. 4(a).

Lee et al. used a thin Si_3N_4/SiO_2 thermal emission layer on an Al foil and obtained cooling at around 11 °C on a smart watch. They first demonstrated a colored passive radiative cooler that possesses structural softness and enables application to flexible devices without affecting the visual esthetics (Fig. 4(b)) [129]. In order to achieve additional potential of radiative coolers for wearable electronics, Zhang et al. obtained a hydrophobic, flexible, and mechanically superior radiative cooling film. By mimicking tropical beetles, they fabricated micropyramid periodic arrayed polydimethylsiloxane (PDMS) encapsulating randomly distributed spherical ceramic particles (e.g., Al_2O_3, TiO_2, and ZnO). The bioinspired radiative cooling film drops the temperature of the skin under direct sunlight by around 5 °C as shown in Fig. 4(c) [46]. In addition to mechanical compliance, substantial progress has been achieved by Xu et al. They created recyclable, self-healing, and breathable on-skin electronics with passive cooling capabilities. The electronics can function

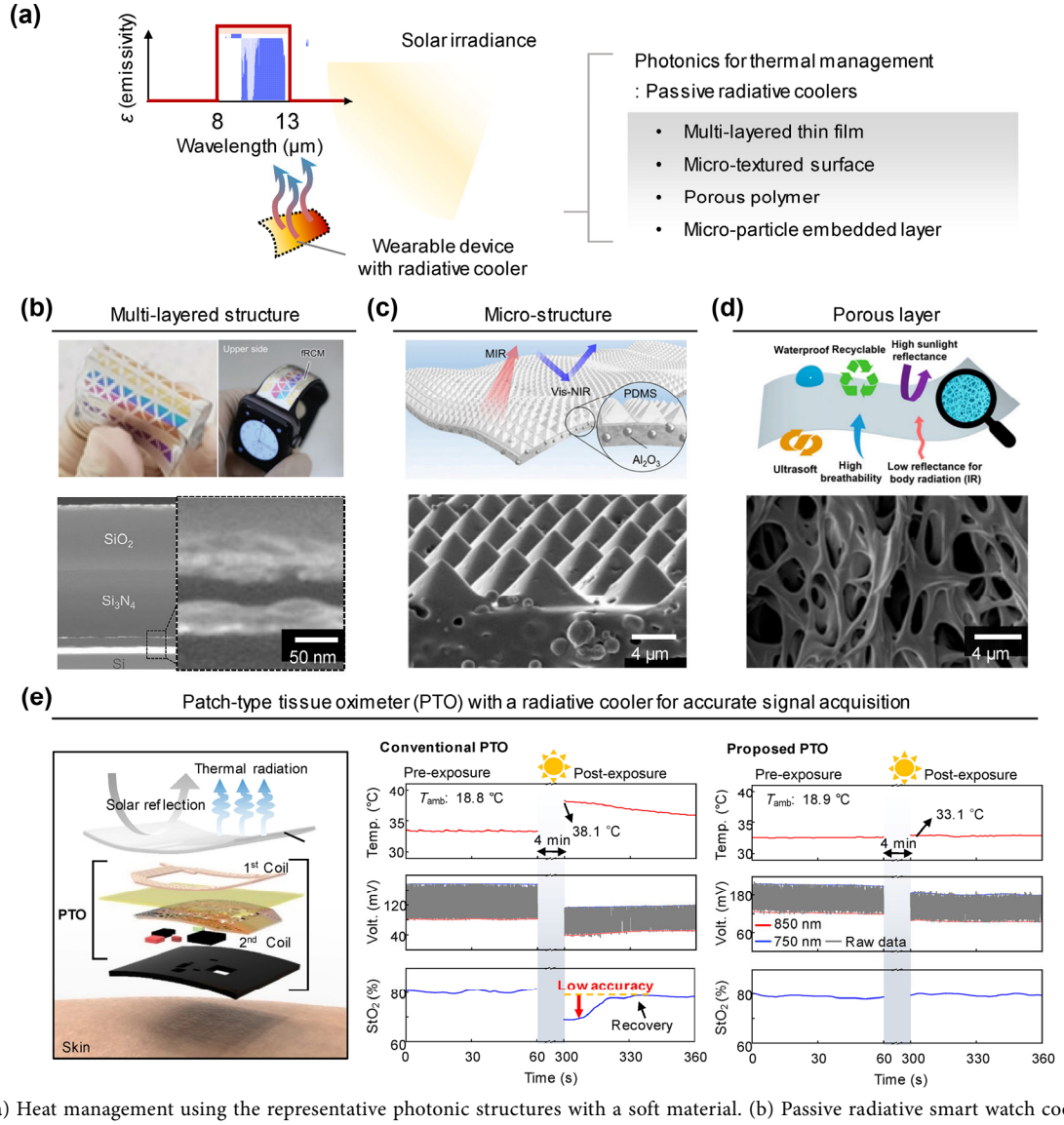

Figure 4 (a) Heat management using the representative photonic structures with a soft material. (b) Passive radiative smart watch cooling using a multilayer structure. Reproduced with permission from Ref. [129], © WILEY-VCH Verlag GmbH & Co. KGaA, Weinheim 2018. (c) Bioinspired cooling film with a micro-textured structure. Reproduced with permission from Ref. [46], © National Academy of Sciences 2020. (d) On-skin electronics with passive cooling capabilities, on a porous polymer substrate. Reproduced with permission from Ref. [30], © National Academy of Sciences 2020. (e) PTO with a radiative cooler for accurate signal acquisition in both indoor and outdoor wearable device applications. Reproduced with permission from Ref. [130], © WILEY-VCH Verlag GmbH & Co. KGaA, Weinheim 2020.

as electrophysiological sensors (temperature, hydration, and pressure) and electrical stimulators, as well as deliver a cooling effect of around 6 °C. The cooling property is inherited from the porous polystyrene-blockpoly(ethylene-ran-butylene)-block-polystyrene (SEBS) substrate, while the multifunctionality is attributed to the simple fabrication method of spray printing (Fig. 4(d)) [30]. The approach is more favorable for the development of future high-throughput electronics as it is simple, inexpensive, scalable, and multifunctional. Further thermal management studies in wearable devices were implemented by Kang et al. They pointed out the importance of accurate signal acquisition during outdoor activities. They proposed a device that is a wireless/battery-free and thermally regulated patch-type tissue oximeter (PTO) with radiative cooling structures, as illustrated in Fig. 4(e) [130]. A combined polymer with nano-/micro-voids (polymethylmethacrylate (PMMA) and SEBS) exhibited a maximized radiative cooling performance of 6 °C below the ambient air temperature. Finally, the proposed PTO device showed stabilized tissue oxygen saturation (StO_2) value even under sunlight exposure as shown in Fig. 5(e)(right). However, the conventional one showed ~ 13% difference of StO_2 value between indoor and outdoor measurement (Fig. 5(e)(middle)). This result initiates basis study for far-reaching goal of wearable monitoring electronics—an accurate signal acquisition at any situation. Various candidate substances for wearables are briefly summarized in Table 2 based on their cooling performance (i.e., cooling temperature and power) [30, 46–48, 129, 131, 132].

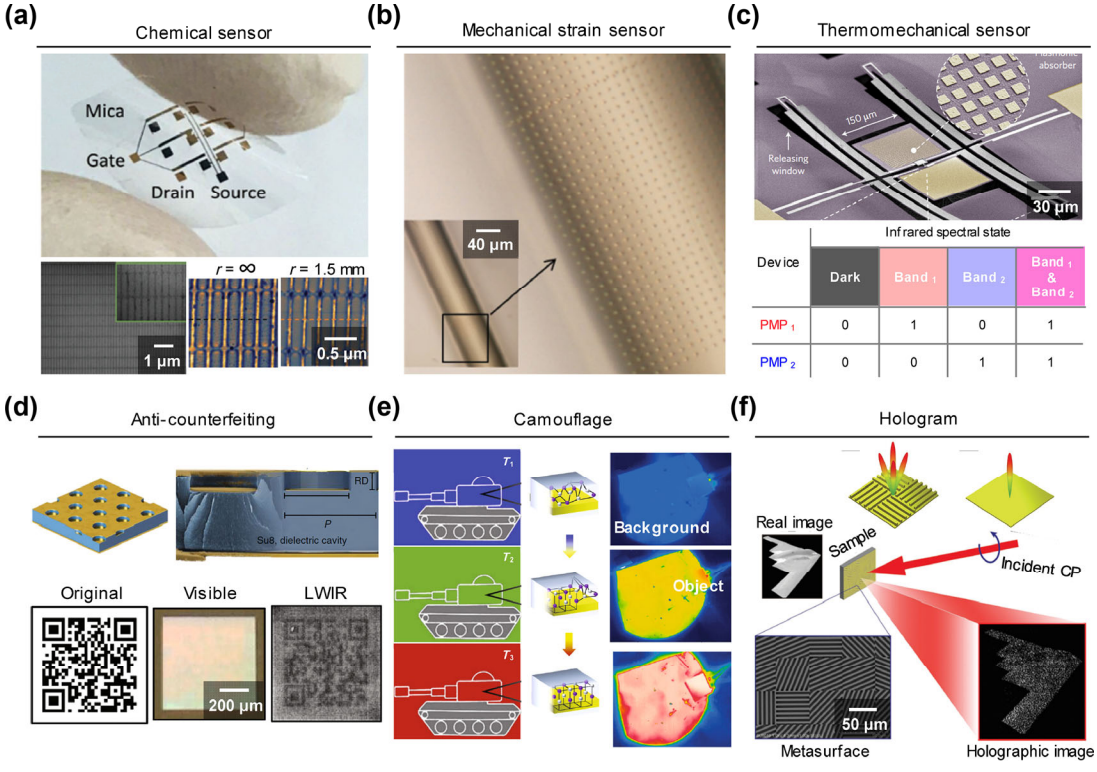

Figure 5 Recent IR regulation study of (a) chemical/pollutant sensor (reproduced with permission from Ref. [152], © WILEY-VCH Verlag GmbH & Co. KGaA, Weinheim 2018), (b) mechanical strain sensor (reproduced with permission from Ref. [141], © WILEY-VCH Verlag GmbH & Co. KGaA, Weinheim 2011), (c) thermomechanical sensor (rproduced with permission from Ref. [119], © National Academy of Sciences 2017), (d) anti-counterfeiting technology (reproduced with permission from Ref. [117], © National Academy of Sciences 2018), (e) camouflage for IR covert wearables (reproduced with permission from Ref. [164], © National Academy of Sciences 2018), and (f) hologram (reproduced with permission from Ref. [121], © WILEY-VCH Verlag GmbH & Co. KGaA, Weinheim 2018).

Table 2 Cooling performance of radiative cooler on flexible substrate

Structure	Material	Cooling power (W/m^2)	Cooling temperature (°C)	Experiment condition	Reference
Multilayer	Ag-SiO_2-Ag Si_3N_4/SiO_2	—	3.9	800 W/m^2 of solar power and 45 °C of ambient	[129]
Microstructure	Al_2O_3 spherical particles in PDMS	90.8	5.1	862 W/m^2 of solar power, 32 °C of ambient, and 22.7% of RH	[46]
Nanotube	SiO_2 amorphous alumina nanotubes on Ag-PDMS	—	4.3	39 °C of ambient	[131]
Membrane	PVDF/TEOS fibers with nanopores and SiO_2 microspheres	61	3.5	Peak solar power of 1,000 W/m^2 and 35 °C of ambient	[47]
Porous film	Hierarchically porous $(VdF\text{-}HFP)_{HP}$	96	6	750 W/m^2 of solar power and 14.5 °C of ambient	[132]
Porous film	SEBS	70	6	840 W/m^2 of solar power	[30]
Porous film	Polyethylene (PE) aerogel	70 ± 14	5–6	Peak solar power over 1,000 W/m^2, 3.5 °C of ambient, and 26% of RH	[48]

4.2 Recent advances and possible applications

Today, the mid- and far-IR spectral range (λ ~ 2–20 μm) is of particular importance because a wide variety of sensing and detection systems are applicable in this range [133, 134]. With the advancements in microfabrication and plasmonics, pioneering progress has motivated various achievements [135–138] in information and communication, medical sciences, defense, chemical and biological sensing, and spectroscopy, among many others. Despite all recent improvements, there are several challenges to be overcome for improving the practical applicability of devices based on IR spectral engineering. In this section, we introduce recent advances in the engineering of plasmonics and provide our perspectives on their potential application for next-generation wearables.

4.2.1 IR sensors

The wavelength range from 3 to 20 μm is known as the "molecular fingerprint" region, because molecules have their fundamental vibration modes in this part of the electromagnetic spectrum [139]. Plasmonic engineering in this region has, thus, been regarded as an effective means for optical analysis of chemical components, with the benefits of (1) providing tunable spectral peaks, (2) having alternative technology solutions, and (3) offering clear operations because sensing is conducted in atmospheric transparency windows ($\lambda \approx$ 3–5 and 8–14 μm), at which strong absorption by dust, greenhouse gases, and water vapor is avoided. However, the design of flexible photonics for plasmonic mid-infrared (MIR) sensors has not yet been widely explored [140–150]. Here, we summarize recent advances in flexible IR sensors accompanied by two-dimensional (2D) materials, IR spectroscopy, nonplanar surfaces, and in-depth understanding of plasmonics.

Yang et al. reported a new hybridized plasmon–phonon polariton mode in a graphene/hexagonal boron nitride (h-BN) material. They explained the plasmonic phenomena as interaction between a highly localized graphene plasmon electromagnetic field and the resonant polarization of the monolayer h-BN lattice [151]. After this report, Hu et al. demonstrated a flexible and electrically tunable plasmonic device with graphene–mica heterostructures based on previous research results. Their device showed different plasmonic resonance frequencies with respect to changing the chemical Fermi level. The resonance frequency, strength, quality factor, electrical tunability, and lifetime of the sensor exhibited no change after 1,000 bending cycles (Fig. 5(a)) [152]. This device can be applied as a chemical sensor for the analysis of toxic agents, air and water pollutants, greenhouse gases, and food and drink products.

MIR sensing also covers analysis of mechanical strain. Aksu et al. demonstrated flexible plasmonics and metamaterials on polymeric substrates. They even patterned plasmonic nanostructures fabricated on thin flexible films, which can be directly transferred and wrapped around nonplanar surfaces, such as optical fibers (Fig. 5(b)) [141]. By patterning plasmonic nanoantennas on stretchable polymer films, the optical responses of the antenna arrays can be actively tuned by mechanical stretching of the flexible substrate. As a result of the mechanical strain applied to the fabricated sample, a 160 nm red-shift of the resonance wavelengths is achieved. The integration of plasmonics and metamaterials on nonplanar surfaces can lead to emerging technologies based on flexible photonics/electronics. The use of wearable devices with IR flexible plasmonic sensors serves as an effective approach for observational human research and continuous monitoring of imperceptible toxic materials from the environment (i.e., such devices allow the detection of signals beyond the visible spectral range). The research scope also includes applications in healthcare. For instance, Chang et al. developed on-chip flexible localized surface plasmon resonance biosensors for the detection of cancer cells on nonplanar surfaces [145]. Another research group fabricated zero-power IR digitizing thermomechanical sensors; see Fig. 5(c) [119]. The device can detect IR spectral signal wavelengths ranging from 3 to 14 μm (e.g., the emission peaks of the heated gases or a burning fire). By using plasmonically enhanced micromechanical photoswitches, the IR-induced temperature rise causes a downward bending of the legs through which signals can be transmitted. The zero-power IR digitizing thermomechanical sensor offers higher sensitivity than the state-of-the-art passive- or active-only thermomechanical sensors as well as overcomes inherent power consumption problems of active sensors.

4.2.2 Anti-counterfeiting of wearable devices

In the last few decades, wireless technology has evolved and facilitated the development of ubiquitous, interconnected platforms for everyday tasks [153, 154]. However, this technology has reliability issues, placing importance on lock and key in order to ensure the authenticity of goods or identities [155–158]. Counterfeiting is one of the major problems that result in user's health and safety failure due to low-quality components. Unawareness makes consumers more vulnerable to threats such as malware, hazardous materials, excessive emissions, or explosions [159]. In addition, counterfeiting is a risk to manufacturers imposing an economic burden on society in all countries [160–162]. Accordingly, developing anti-counterfeiting techniques has become an important challenge that can be overcome through advanced photonic approaches.

Franklin et al. demonstrated a multispectral encoding system for anti-counterfeiting. They fabricated large-area cavity-coupled plasmonic materials with tunable absorption throughout the mid (3–5 μm) and far (8–12 μm) IR waves. By tailoring the plasmonic structures to maximize the diffraction efficiency, they implemented a multispectral Quick Response (QR) code, where images, viewable in the IR spectral domain, are hidden in the visible domain (Fig. 5(d)) [117]. Lee et al. also suggested spatially selective emitters based on spoof surface plasmons to obtain IR anti-counterfeiting. They designed the intriguing emission features of a selective emitter consisting of a Ag corrugated pattern on a Si substrate and an IR-transparent encapsulating layer, i.e., SEBS. Thermal imaging resulted in the detection of hidden patterns only in the case of the sample with the SEBS superstrate, wherein plasmonics existed [118]. These IR microtagging technologies are expected to contribute to the authentication of secure mobile devices without hindering the visual esthetics of wearables.

4.2.3 Camouflage for IR covert wearables

Visually imperceptive human assistive devices can provide new functionalities for serving the user's rehabilitation process or supporting disabled parts in the body without discomfort, altering biomechanics, and obstruction to others. As a supportive component, camouflage aims to allow for invisibility to adapt to the natural environment or humans [163]. As an object can be perceived because of its unique signature of multiple electromagnetic fields, thermal camouflage regulates IR radiation [114, 122–124, 164–167].

The earliest camouflage machine was created by scientists at Harvard University and Defense Advanced Research Projects Agency (DARPA). They implemented visible and IR camouflage by changing the color and pattern of microfluidic networks with a compressed-air source [168]. Zero-power stealth was also realized by stimulus-responsive photonic engineering

[116, 123, 164]. $Ge_2Sb_2Te_5$ (GST) is a well-known phase-change material, which shows the emissivity difference between the amorphous and crystalline phases within a broad IR wavelength region (4–12.5 μm) [169]. Qu et al. developed GST-based devices to match the emissivity of a given object and background and achieved thermal camouflage for background temperatures ranging from 30 to 50 °C (Fig. 5(e)) [164]. Recent achievements using no energy for IR camouflage empower applications in transparent systems, undercover operations, and soft covert wearables.

4.2.4 *Holograms for observation in hostile environment*

Holography is an interference method of recording/decoding the light waves diffracted by a subject illuminated with coherent light [170]. In most cases, holography is applied in the visible range as people prefer to see their beams, e.g., during optical alignment. However, holography at non-visible wavelengths (i.e., long-wave infrared (LWIR) ranging from 8 to 15 μm) has various advantages. The most obvious one is the decrease in the sensitivity of the holographic setup by reducing vibration and seismic noise compared to the visible wavelength [171]. This makes LWIR holography more advisable in various fields such as nondestructive testing [172], aerospace [173–176], and cultural heritage [177, 178]. Remarkably, LWIR holography finds application safety insurance as well, where it can be used to see through smoke and flames [179]. In this subsection, we discuss the ubiquitous modern approach of holograms for observing hostile environments in which smoke, flames, and dust impair visibility [180].

An original application of LWIR holography to reconstruct a scene or an object located behind or inside smoke has been proposed by Locatelli et al. [179]. They note that CO_2 and H_2O gases absorb at some wavelengths, which are different from the emission lines of the CO_2 laser. Therefore, an interference laser setup based on such lasers could record a hologram of objects that is not visible through such gases. Recent advances in nanotechnology and fabrication enable the continuous evolution of optical metasurface-based holography [181]. Larouche et al. demonstrated a multilayer, lithographically patterned metal element, phase hologram in the IR region (10.6 μm). The metamaterial used in their work consisted of gold discs. The polarizability of distinct gold discs increases with the size of the metallic inclusions. Xie et al. suggested a simpler metasurface-based hologram with enhanced mechanical properties for more applications on wearables. They fabricated ultrathin holographic metasurfaces with high strength, flexibility, and ductility. The sample simultaneously produces ultralow specular reflection and far-IR emission (8–14 μm) by combining the low emission nature of metal and the photonic spin–orbit interaction in spatially inhomogeneous structures. The elaborated design can lead to the reconstruction of the wave front and obtain holographic images at a wavelength of 10.6 μm (Fig. 5(f)) [121], which has potential applications in wearable displays, image storage, and image replication, even in hostile environments.

5 Conclusion

The interaction of natural creatures with surrounding environments has been offering scientists great inspiration to develop novel photonic structures. These structures have practical applications for sensing, heat management, and investigation of some ubiquitous advances for human endeavor. The structures at the wavelength scale enable the management of a wide range of electromagnetic spectra. Butterflies and beetles with hundreds-of-nanometers-sized structures show brilliant colors depending on the surrounding environment, while the Saharan silver ant and tropical beetles having surfaces with combination of micro- and nanometer compositions exhibit independent control of light and heat. In this review article, we have covered various studies focused on the light–matter interaction, from the ultraviolet to far-IR spectrum. Some practical applications are included in specific spectral range, however, the achievements exist across the overall range of electromagnetic spectrum. One can expect to apply the engineering method of light waves in one domain to another, thanks to the beauty of Maxwell's equation.

Wearable/flexible devices are becoming more streamlined in the form of patches or skins that harmonize with the wearer's daily life. Some of these devices require functional structures for external interactions to provide adaptive internal care in response to the external environment. Future wearable/flexible devices will be able to monitor a wide range of external stimuli in real time, enabling by proactive medical diagnosis and prevention towards ultimate goal, respect for life. In addition, it will guarantee safety and happiness of the people with applying most recent advanced design from various research fields. The photonic engineering is regarded as breakthrough tool for traditional material limitations. Indeed, a lot of works have verified and shown the materials beyond its natural aspect [182–187]. However, practical appliance of the achievements on wearable devices have been emerging to tackle some of the critical challenges rooted in 1) modeling complicity, 2) fabrication infeasibility or 3) unavailability of device integration. For instance, 1) the evolution of photonic-based sensors ask more elaborated design to improve its sensitivity, which could also result in 2) inaccurate match between the design and fabrication. Also, 3) the need for a complex interferometric geometry for recording/decoding holographic image [171, 172, 188] could be included critical issue for on-field wearable application.

To accommodate the full potential of such external photonic structures on miniaturized flexible/wearable devices, smart algorithms/strategies, procedural design and additional theoretical tool should be developed. Meanwhile, in order to be attached to the human body and to be utilized, manufacturing on various surfaces and shapes is required, so that integration of organic/inorganic components, durability against repetitive deformation and external environments must be verified. Finally, as practical device integration requires light, low-cost, and uncomplicated setup, the multimodality and interdisciplinary approaches are needed to overcome a fundamental limit exist in classic research fields. This review article deals with only the tip of iceberg of the vast field of wearable device related photonics, while unsolved problems continue to exist, which stimulates our imagination for the development of new systems. We appreciate a bunch of research approaches are left in the field of photonic structures based on wearable related techniques. Given the wide variety of innovative studies and tremendous commercial opportunities for wearable devices, we look forward to exciting new developments for external/internal care systems in the near future. Beyond the challenges, the commercial application of wearable devices is expected to grow rapidly and will facilitate changing and improving people's lives.

Acknowledgements

This work was supported by the National Research Foundation of Korea (Nos. NRF-2020R1A2C2004983, NRF2018M3D1A1058997, and NRF-2018R1A4A1025623). This work was also supported by the GIST Research Institute (GRI) grant funded by the GIST in 2020 and the Korea Institute of Energy Technology Evaluation and Planning (KETEP) and by the Ministry of

Trade, Industry, and Energy (MOTIE) of the Republic of Korea (No. 20183010014310). This work was partly supported by Institute of Information & communications Technology Planning & Evaluation (IITP) grant funded by the Korea government (MSIT) (No. 2020-0-01000, Light field and LiDAR sensor fusion systems for full self-driving).

References

[1] Xu, S.; Zhang, Y. H.; Jia, L.; Mathewson, K. E.; Jang, K. I.; Kim, J.; Fu, H. R.; Huang, X.; Chava, P.; Wang, R. H. et al. Soft microfluidic assemblies of sensors, circuits, and radios for the skin. *Science* **2014**, *344*, 70–74.

[2] Kim, D. H.; Lu, N. S.; Ma, R.; Kim, Y. S.; Kim, R. H.; Wang, S. D.; Wu, J.; Won, S. M.; Tao, H.; Islam, A. et al. Epidermal electronics. *Science* **2011**, *333*, 838–843.

[3] Son, D.; Lee, J.; Qiao, S. T.; Ghaffari, R.; Kim, J.; Lee, J. E.; Song, C.; Kim, S. J.; Lee, D. J.; Jun, S. W. et al. Multifunctional wearable devices for diagnosis and therapy of movement disorders. *Nat. Nanotechnol.* **2014**, *9*, 397–404.

[4] Hong, Y. J.; Lee, H.; Kim, J.; Lee, M.; Choi, H. J.; Hyeon, T.; Kim, D. H. Multifunctional wearable system that integrates sweat-based sensing and vital-sign monitoring to estimate pre-/post-exercise glucose levels. *Adv. Funct. Mater.* **2018**, *28*, 1805754.

[5] Zhao, D. W.; Zhu, Y.; Cheng, W. K.; Xu, G. W.; Wang, Q. W.; Liu, S. X.; Li, J.; Chen, C. J.; Yu, H. P.; Hu, L. B. A dynamic gel with reversible and tunable topological networks and performances. *Matter* **2020**, *2*, 390–403.

[6] Chen, S. M.; Gao, H. L.; Sun, X. H.; Ma, Z. Y.; Ma, T.; Xia, J.; Zhu, Y. B.; Zhao, R.; Yao, H. B.; Wu, H. A. et al. Superior biomimetic nacreous bulk nanocomposites by a multiscale soft-rigid dual-network interfacial design strategy. *Matter* **2019**, *1*, 412–427.

[7] Kang, J. H.; Son, D. H.; Wang, G. J. N.; Liu, Y. X.; Lopez, J.; Kim, Y.; Oh, J. Y.; Katsumata, T.; Mun, J.; Lee, Y. et al. Tough and water-insensitive self-healing elastomer for robust electronic skin. *Adv. Mater.* **2018**, *30*, 1706846.

[8] Sung, S. H.; Kim, Y. S.; Joe, D. J.; Mun, B. H.; You, B. K.; Hahn, S. K.; Berggren, M.; Kim, D.; Lee, K. J. Flexible wireless powered drug delivery system for targeted administration on cerebral cortex. *Nano Energy* **2018**, *51*, 102–112.

[9] Jang, K. I.; Han, S. Y.; Xu, S.; Mathewson, K. E.; Zhang, Y. H.; Jeong, J. W.; Kim, G. T.; Webb, R. C.; Lee, J. W.; Dawidczyk, T. J. et al. Rugged and breathable forms of stretchable electronics with adherent composite substrates for transcutaneous monitoring. *Nat. Commun.* **2014**, *5*, 4779.

[10] Kim, T. I.; McCall, J. G.; Jung, Y. H.; Huang, X.; Siuda, E. R.; Li, Y. H.; Song, J. Z.; Song, Y. M.; Pao, H. A.; Kim, R. H. et al. Injectable, cellular-scale optoelectronics with applications for wireless optogenetics. *Science* **2013**, *340*, 211–216.

[11] Koh, A.; Kang, D.; Xue, Y. G.; Lee, S.; Pielak, R. M.; Kim, J.; Hwang, T.; Min, S.; Banks, A.; Bastien, P. et al. A soft, wearable microfluidic device for the capture, storage, and colorimetric sensing of sweat. *Sci. Trans. Med.* **2016**, *8*, 366ra165.

[12] Kim, J.; Gutruf, P.; Chiarelli, A. M.; Heo, S. Y.; Cho, K.; Xie, Z. Q.; Banks, A.; Han, S.; Jang, K. I.; Lee, J. W. et al. Miniaturized battery-free wireless systems for wearable pulse oximetry. *Adv. Funct. Mater.* **2017**, *27*, 1604373.

[13] Seshadri, D. R.; Li, R. T.; Voos, J. E.; Rowbottom, J. R.; Alfes, C. M.; Zorman, C. A.; Drummond, C. K. Wearable sensors for monitoring the physiological and biochemical profile of the athlete. *npj Digit. Med.* **2019**, *2*, 72.

[14] Heikenfeld, J.; Jajack, A.; Feldman, B.; Granger, S. W.; Gaitonde, S.; Begtrup, G.; Katchman, B. A. Accessing analytes in biofluids for peripheral biochemical monitoring. *Nat. Biotechnol.* **2019**, *37*, 407–419.

[15] Lim, H. R.; Kim, H. S.; Qazi, R.; Kwon, Y. T.; Jeong, J. W.; Yeo, W. H. Advanced soft materials, sensor integrations, and applications of wearable flexible hybrid electronics in healthcare, energy, and environment. *Adv. Mater.* **2020**, *32*, 1901924.

[16] Xu, X.; Chen, J.; Cai, S.; Long, Z.; Zhang, Y.; Su, L.; He, S.; Tang, C.; Liu, P.; Peng, H. A real-time wearable UV-radiation monitor based on a high-performance p-CuZnS/n-TiO_2 photodetector. *Adv. Mater.* **2018**, *30*, 1803165.

[17] Jang, K. I.; Li, K.; Chung, H. U.; Xu, S.; Jung, H. N.; Yang, Y. Y.; Kwak, J. W.; Jung, H. H.; Song, J.; Yang, C. et al. Self-assembled three dimensional network designs for soft electronics. *Nat. Commun.* **2017**, *8*, 15894.

[18] Yao, J. D.; Yang, G. W. Flexible and high-performance all-2D photodetector for wearable devices. *Small* **2018**, *14*, 1704524.

[19] Choi, J.; Bandodkar, A. J.; Reeder, J. T.; Ray, T. R.; Turnquist, A.; Kim, S. B.; Nyberg, N.; Hourlier-Fargette, A.; Model, J. B.; Aranyosi, A. J. Soft, skin-integrated multifunctional microfluidic systems for accurate colorimetric analysis of sweat biomarkers and temperature. *ACS Sens.* **2019**, *4*, 379–388.

[20] Cai, Z. Y.; Smith, N. L.; Zhang, J. T.; Asher, S. A. Two-dimensional photonic crystal chemical and biomolecular sensors. *Anal. Chem.* **2015**, *87*, 5013–5025.

[21] Yamamoto, Y.; Yamamoto, D.; Takada, M.; Naito, H.; Arie, T.; Akita, S.; Takei, K. Efficient skin temperature sensor and stable gel-less sticky ECG sensor for a wearable flexible healthcare patch. *Adv. Healthc. Mater.* **2017**, *6*, 1700495.

[22] Tsuchiya, M.; Kurashina, Y.; Onoe, H. Eye-recognizable and repeatable biochemical flexible sensors using low angle-dependent photonic colloidal crystal hydrogel microbeads. *Sci. Rep.* **2019**, *9*, 17059.

[23] Zheng, Z. Q.; Yao, J. D.; Wang, B.; Yang, G. W. Light-controlling, flexible and transparent ethanol gas sensor based on ZnO nanoparticles for wearable devices. *Sci. Rep.* **2015**, *5*, 11070.

[24] Shafiee, H.; Lidstone, E. A.; Jahangir, M.; Inci, F.; Hanhauser, E.; Henrich, T. J.; Kuritzkes, D. R.; Cunningham, B. T.; Demirci, U. Nanostructured optical photonic crystal biosensor for HIV viral load measurement. *Sci. Rep.* **2014**, *4*, 4116.

[25] Lee, N.; Wang, C.; Park, J. User-friendly point-of-care detection of influenza a (H1N1) virus using light guide in three-dimensional photonic crystal. *RSC Adv.* **2018**, *8*, 22991–22997.

[26] Wang, F.; Gopinath, S. C. B.; Lakshmipriya, T. Aptamer-antibody complementation on multiwalled carbon nanotube-gold transduced dielectrode surfaces to detect pandemic swine influenza virus. *Int. J. Nanomed.* **2019**, *14*, 8469–8481.

[27] Choe, A.; Yeom, J.; Shanker, R.; Kim, M. P.; Kang, S.; Ko, H. Stretchable and wearable colorimetric patches based on thermoresponsive plasmonic microgels embedded in a hydrogel film. *NPG Asia Mater.* **2018**, *10*, 912–922.

[28] Hong, S.; Gu, Y.; Seo, J. K.; Wang, J.; Liu, P.; Meng, Y. S.; Xu, S.; Chen, R. K. Wearable thermoelectrics for personalized thermoregulation. *Sci. Adv.* **2019**, *5*, eaaw0536.

[29] Malakooti, M. H.; Kazem, N.; Yan, J. J.; Pan, C. F.; Markvicka, E. J.; Matyjaszewski, K.; Majidi, C. Liquid metal supercooling for low-temperature thermoelectric wearables. *Adv. Funct. Mater.* **2019**, *29*, 1906098.

[30] Xu, Y. D.; Sun, B. H.; Ling, Y.; Fei, Q. H.; Chen, Z. Y.; Li, X. P.; Guo, P. J.; Jeon, N.; Goswami, S.; Liao, Y. X. et al. Multiscale porous elastomer substrates for multifunctional on-skin electronics with passive-cooling capabilities. *Proc. Natl. Acad. Sci. USA* **2020**, *117*, 205–213.

[31] Hawkeye, M. M.; Brett, M. J. Optimized colorimetric photonic-crystal humidity sensor fabricated using glancing angle deposition. *Adv. Funct. Mater.* **2011**, *21*, 3652–3658.

[32] Ye, B. F.; Rong, F.; Gu, H. C.; Xie, Z. Y Cheng, Y.; Zhao, Y. J.; Gu, Z. Z. Bioinspired angle-independent photonic crystal colorimetric sensing. *Chem. Commun.* **2013**, *49*, 5331–5333.

[33] Ye, B. F.; Ding, H. B.; Cheng, Y.; Gu, H. C.; Zhao, Y. J.; Xie, Z. Y.; Gu, Z. Z. Photonic crystal microcapsules for label-free multiplex detection. *Adv. Mater.* **2014**, *26*, 3270–3274.

[34] Qin, M.; Sun, M.; Bai, R. B.; Mao, Y. Q.; Qian, X. S.; Sikka, D.; Zhao, Y.; Qi, H. J.; Suo, Z. G.; He, X. M. Bioinspired hydrogel interferometer for adaptive coloration and chemical sensing. *Adv. Mater.* **2018**, *30*, 1800468.

[35] Holtz, J. H.; Asher, S. A. Polymerized colloidal crystal hydrogel films as intelligent chemical sensing materials. *Nature* **1997**, *389*, 829–832.

[36] Saito, H.; Takeoka, Y.; Watanabe, M. Simple and precision design of porous gel as a visible indicator for ionic species and concentration. *Chem. Commun.* **2003**, 2126–2127.

[37] Lim, H. S.; Lee, J. H.; Walish, J. J.; Thomas, E. L. Dynamic swelling of tunable full-color block copolymer photonic gels via counterion exchange. *ACS Nano* **2012**, *6*, 8933–8939.
[38] Lova, P.; Manfredi, G.; Boarino, L.; Comite, A.; Laus, M.; Patrini, M.; Marabelli, F.; Soci, C.; Comoretto, D. Polymer distributed Bragg reflectors for vapor sensing. *ACS Photonics* **2015**, *2*, 537–543.
[39] Kim, C.; Lee, H.; Devaraj, V.; Kim, W. G.; Lee, Y.; Kim, Y.; Jeong, N. N.; Choi, E. J.; Baek, S. H.; Han, D. W. et al. Hierarchical cluster analysis of medical chemicals detected by a bacteriophage-based colorimetric sensor array. *Nanomaterials* **2020**, *10*, 121.
[40] Oh, H. J.; Yeang, B. J.; Park, Y. K.; Choi, H. J.; Kim, J. H.; Kang, Y. S.; Bae, Y.; Kim, J. Y.; Lim, S. J.; Lee, W. Washable colorimetric nanofiber nonwoven for ammonia gas detection. *Polymers* **2020**, *12*, 1585.
[41] Chi, H.; Ze, L. J.; Zhou, X. M.; Wang, F. K. Go film on flexible substrate: An approach to wearable colorimetric humidity sensor. *Dyes Pigm.* **2021**, *185*, 108916.
[42] Qin, M.; Sun, M.; Hua, M. T.; He, X. M. Bioinspired structural color sensors based on responsive soft materials. *Curr. Opin. Solid State Mater. Sci.* **2019**, *23*, 13–27.
[43] Choi, J.; Hua, M.; Lee, S. Y.; Jo, W.; Lo, C. Y.; Kim, S. H.; Kim, H. T.; He, X. M. Hydrocipher: Bioinspired dynamic structural color-based cryptographic surface. *Adv. Opt. Mater.* **2020**, *8*, 1901259.
[44] Fathi, F.; Rashidi, M. R.; Pakchin, P. S.; Ahmadi-Kandjani, S.; Nikniazi, A. Photonic crystal based biosensors: Emerging inverse opals for biomarker detection. *Talanta* **2021**, *221*, 121615.
[45] Li, D.; Liu, X.; Li, W.; Lin, Z. H.; Zhu, B.; Li, Z. Z.; Li, J. L.; Li, B.; Fan, S. H.; Xie, J. W. et al. Scalable and hierarchically designed polymer film as a selective thermal emitter for high-performance all-day radiative cooling. *Nat. Nanotechnol.* **2021**, *16*, 153–158.
[46] Zhang, H. W.; Ly, K. C. S.; Liu, X. H.; Chen, Z. H.; Yan, M.; Wu, Z. L.; Wang, X.; Zheng, Y. B.; Zhou, H.; Fan, T. X. Biologically inspired flexible photonic films for efficient passive radiative cooling. *Proc. Natl. Acad. Sci. USA* **2020**, *117*, 14657–14666.
[47] Wang, X.; Liu, X. H.; Li, Z. Y.; Zhang, H. W.; Yang, Z. W.; Zhou, H.; Fan, T. X. Scalable flexible hybrid membranes with photonic structures for daytime radiative cooling. *Adv. Funct. Mater.* **2020**, *30*, 1907562.
[48] Yang, M.; Zou, W. Z.; Guo, J.; Qian, Z. C.; Luo, H.; Yang, S. J.; Zhao, N.; Pattelli, L.; Xu, J.; Wiersma, D. S. Bioinspired "skin" with cooperative thermo-optical effect for daytime radiative cooling. *ACS Appl. Mater. Interfaces* **2020**, 12 , 25286–25293.
[49] Zhu, H. Z.; Li, Q.; Zheng, C. Q.; Hong, Y.; Xu, Z. Q.; Wang, H.; Shen, W. D.; Kaur, S.; Ghosh, P.; Qiu, M. High-temperature infrared camouflage with efficient thermal management. *Light Sci. Appl.* **2020**, *9*, 60.
[50] Park, C.; Kim, J.; Hahn, J. W. Selective emitter with engineered anisotropic radiation to minimize dual-band thermal signature for infrared stealth technology. *ACS Appl. Mater. Interfaces* **2020**, *12*, 43090–43097.
[51] Zhu, H. Z.; Li, Q.; Tao, C. N.; Hong, Y.; Xu, Z. Q.; Shen, W. D.; Kaur, S.; Ghosh, P.; Qiu, M. Multispectral camouflage for infrared, visible, lasers and microwave with radiative cooling. 2020, DOI: 10.21203/rs.3.rs-40658/v1. Research Square. https://www.researchsquare.com/article/rs-40658/v1 (accessed Dec 28, 2020).
[52] Pan, M. Y.; Huang, Y.; Li, Q.; Luo, H.; Zhu, H. Z.; Kaur, S.; Qiu, M. Multi-band middle-infrared-compatible camouflage with thermal management via simple photonic structures. *Nano Energy* **2020**, *69*, 104449.
[53] Xiao, L.; Ma, H.; Liu, J. K.; Zhao, W.; Jia, Y.; Zhao, Q.; Liu, K.; Wu, Y.; Wei, Y.; Fan, S. S. et al. Fast adaptive thermal camouflage based on flexible VO_2/graphene/cnt thin films. *Nano Lett.* **2015**, *15*, 8365–8370.
[54] Kim, J.; Campbell, A. S.; De Ávila, B. E. F.; Wang, J. Wearable biosensors for healthcare monitoring. *Nat. Biotechnol.* **2019**, *37*, 389–406.
[55] Ghaffari, R.; Choi, J.; Raj, M. S.; Chen, S. L.; Lee, S. P.; Reeder, J. T.; Aranyosi, A. J.; Leech, A.; Li, W. H.; Schon, S. et al. Soft wearable systems for colorimetric and electrochemical analysis of biofluids. *Adv. Funct. Mater.* **2020**, *30*, 1907269.
[56] Someya, T.; Amagai, M. Toward a new generation of smart skins. *Nat. Biotechnol.* **2019**, *37*, 382–388.
[57] Lee, G. H.; Moon, H.; Kim, H.; Lee, G. H.; Kwon, W.; Yoo, S.; Myung, D.; Yun, S. H.; Bao, Z. N.; Hahn, S. K. Multifunctional materials for implantable and wearable photonic healthcare devices. *Nat. Rev. Mater.* **2020**, *5*, 149–165.
[58] Gao, Y. J.; Yu, L. T.; Yeo, J. C.; Lim, C. T. Flexible hybrid sensors for health monitoring: Materials and mechanisms to render wearability. *Adv. Mater.* **2020**, *32*, 1902133.
[59] Bandodkar, A. J.; Jeerapan, I.; Wang, J. Wearable chemical sensors: Present challenges and future prospects. *ACS Sens.* **2016**, *1*, 464–482.
[60] Kim, J.; Campbell, A. S.; Wang, J. Wearable non-invasive epidermal glucose sensors: A review. *Talanta* **2018**, *177*, 163–170.
[61] Bandodkar, A. J.; Wang, J. Non-invasive wearable electrochemical sensors: A review. *Trends Biotechnol.* **2014**, *32*, 363–371.
[62] Bandodkar, A. J.; Jia, W. Z.; Wang, J. Tattoo-based wearable electrochemical devices: A review. *Electroanalysis* **2015**, *27*, 562–572.
[63] Campbell, A. S.; Kim, J.; Wang, J. Wearable electrochemical alcohol biosensors. *Curr. Opin Electrochem.* **2018**, *10*, 126–135.
[64] Jia, W. Z.; Bandodkar, A. J.; Valdés-Ramirez, G.; Windmiller, J. R.; Yang, Z. J.; Ramírez, J.; Chan, G.; Wang, J. Electrochemical tattoo biosensors for real-time noninvasive lactate monitoring in human perspiration. *Anal. Chem.* **2013**, *85*, 6553–6560.
[65] Bandodkar, A. J.; Hung, V. W. S.; Jia, W. Z.; Valdés-Ramírez, G.; Windmiller, J. R.; Martinez, A. G.; Ramírez, J.; Chan, G.; Kerman, K.; Wang, J. Tattoo-based potentiometric ion-selective sensors for epidermal pH monitoring. *Analyst* **2013**, *138*, 123–128.
[66] Guinovart, T.; Bandodkar, A. J.; Windmiller, J. R.; Andrade, F. J.; Wang, J. A potentiometric tattoo sensor for monitoring ammonium in sweat. *Analyst* **2013**, *138*, 7031–7038.
[67] Kim, J.; De Araujo, W. R.; Samek, I. A.; Bandodkar, A. J.; Jia, W. Z.; Brunetti, B.; Paixão, T. R. L. C.; Wang, J. Wearable temporary tattoo sensor for real-time trace metal monitoring in human sweat. *Electrochem. Commun.* **2015**, *51*, 41–45.
[68] Kim, J.; Jeerapan, I.; Imani, S.; Cho, T. N.; Bandodkar, A.; Cinti, S.; Mercier, P. P.; Wang, J. Noninvasive alcohol monitoring using a wearable tattoo-based iontophoretic-biosensing system. *ACS Sens.* **2016**, *1*, 1011–1019.
[69] Bandodkar, A. J.; Jeang, W. J.; Ghaffari, R.; Rogers, J. A. Wearable sensors for biochemical sweat analysis. *Ann. Rev. Anal. Chem.* **2019**, *12*, 1–22.
[70] Mayer, M.; Baeumner, A. J. A megatrend challenging analytical chemistry: Biosensor and chemosensor concepts ready for the internet of things. *Chem. Rev.* **2019**, *119*, 7996–8027.
[71] Zhai, Q.; Cheng, W. Soft and stretchable electrochemical biosensors. *Mater. Today Nano* **2019**, *7*, 100041.
[72] Bariya, M.; Nyein, H. Y. Y.; Javey, A. Wearable sweat sensors. *Nat. Electron.* **2018**, *1*, 160–171.
[73] Choi, J.; Ghaffari, R.; Baker, L. B.; Rogers, J. A. Skin-interfaced systems for sweat collection and analytics. *Sci. Adv.* **2018**, *4*, eaar3921.
[74] Nakata, S.; Arie, T.; Akita, S.; Takei, K. Wearable, flexible, and multifunctional healthcare device with an ISFET chemical sensor for simultaneous sweat pH and skin temperature monitoring. *ACS Sens.* **2017**, *2*, 443–448.
[75] Yun, S. H.; Kwok, S. J. J. Light in diagnosis, therapy and surgery. *Nat. Biomed Eng* **2017**, *1*, 0008.
[76] Van Soest, G.; Regar, E.; Van Der Steen, A. F. W. Photonics in cardiovascular medicine. *Nat. Photon.* **2015**, *9*, 626–629.
[77] Kim, H.; Beack, S.; Han, S.; Shin, M.; Lee, T.; Park, Y.; Kim, K. S.; Yetisen, A. K.; Yun, S. H.; Kwon, W. et al. Multifunctional photonic nanomaterials for diagnostic, therapeutic, and theranostic applications. *Adv. Mater.* **2018**, *30*, 1701460.
[78] Yokota, T.; Zalar, P.; Kaltenbrunner, M.; Jinno, H.; Matsuhisa, N.; Kitanosako, H.; Tachibana, Y.; Yukita, W.; Koizumi, M.; Someya, T. Ultraflexible organic photonic skin. *Sci. Adv.* **2016**, *2*, e1501856.
[79] Shao, J. D.; Xie, H. H.; Huang, H.; Li, Z. B.; Sun, Z. B.; Xu, Y. H.; Xiao, Q. L.; Yu, X. F.; Zhao, Y. T.; Zhang, H. et al. Biodegradable black phosphorus-based nanospheres for *in vivo* photothermal cancer therapy. *Nat. Commun.* **2016**, *7*, 12967.
[80] Liu, K.; Xing, R. R.; Zou, Q. L.; Ma, G. H.; Möhwald, H.; Yan, X. H. Simple peptide-tuned self-assembly of photosensitizers towards anticancer photodynamic therapy. *Angew. Chem.* **2016**, *128*, 3088–3091.
[81] Hamblin, M. R.; Huang, Y. Y.; Heiskanen, V. Non-mammalian hosts and photobiomodulation: Do all life-forms respond to light? *Photochem Photobiol* **2019**, *95*, 126–139.

[82] Kim, J. H.; Moon, J. H.; Lee, S. Y.; Park, J. Biologically inspired humidity sensor based on three-dimensional photonic crystals. *Appl. Phys. Lett.* **2010**, *97*, 103701.
[83] Potyrailo, R. A.; Bonam, R. K.; Hartley, J. G.; Starkey, T. A.; Vukusic, P.; Vasudev, M.; Bunning, T.; Naik, R. R.; Tang, Z. X.; Palacios, M. A. Towards outperforming conventional sensor arrays with fabricated individual photonic vapour sensors inspired by *Morpho* butterflies. *Nat. Commun.* **2015**, *6*, 7959.
[84] Fu, T.; Zhao, X.; Chen, L.; Wu, W. S.; Zhao, Q.; Wang, X. L.; Guo, D. M.; Wang, Y. Z. Bioinspired color changing molecular sensor toward early fire detection based on transformation of phthalonitrile to phthalocyanine. *Adv. Funct. Mater.* **2019**, *29*, 1806586.
[85] Liu, F. F.; Shan, B.; Zhang, S. F.; Tang, B. T. SnO_2 inverse opal composite film with low-angle-dependent structural color and enhanced mechanical strength. *Langmuir* **2018**, *34*, 3918–3924.
[86] Bae, K.; Lee, J.; Kang, G. M.; Yoo, D. S.; Lee, C. W.; Kim, K. Refractometric and colorimetric index sensing by a plasmon-coupled hybrid AAO nanotemplate. *RSC Adv.* **2015**, *5*, 103052–103059.
[87] Duan, X. Y.; Liu, N. Scanning plasmonic color display. *ACS Nano* **2018**, *12*, 8817–8823.
[88] Chung, K.; Yu, S.; Heo, C. J.; Shim, J. W.; Yang, S. M.; Han, M. G.; Lee, H. S.; Jin, Y.; Lee, S. Y.; Park, N. Flexible, angle-independent, structural color reflectors inspired by morpho butterfly wings. *Adv. Mater.* **2012**, *24*, 2375–2379.
[89] Fu, F. F.; Shang, L. R.; Chen, Z. Y.; Yu, Y. R.; Zhao, Y. J. Bioinspired living structural color hydrogels. *Sci. Robot.* **2018**, *3*, eaar8580.
[90] Zhong, K.; Liu, L. W.; Lin, J. Y.; Li, J. Q.; Van Cleuvenbergen, S.; Brullot, W.; Bloemen, M.; Song, K.; Clays, K. Bioinspired robust sealed colloidal photonic crystals of hollow microspheres for excellent repellency against liquid infiltration and ultrastable photonic band gap. *Adv. Mater. Interfaces* **2016**, *3*, 1600579.
[91] Kurland, N. E.; Dey, T.; Kundu, S. C.; Yadavalli, V. K. Precise patterning of silk microstructures using photolithography. *Adv. Mater.* **2013**, *25*, 6207–6212.
[92] Liu, W. P.; Zhou, Z. T.; Zhang, S. Q.; Shi, Z. F.; Tabarini, J.; Lee, W.; Zhang, Y. S.; Corder, S. N. G.; Li, X. X.; Dong, F. et al. Precise protein photolithography (p^3): High performance biopatterning using silk fibroin light chain as the resist. *Adv. Sci.* **2017**, *4*, 1700191.
[93] Wang, Y.; Aurelio, D.; Li, W. Y.; Tseng, P.; Zheng, Z. Z.; Li, M.; Kaplan, D. L.; Liscidini, M.; Omenetto, F. G. Modulation of multiscale 3D lattices through conformational control: Painting silk inverse opals with water and light. *Adv. Mater.* **2017**, *29*, 1702769.
[94] Kats, M. A.; Blanchard, R.; Genevet, P.; Capasso, F. Nanometre optical coatings based on strong interference effects in highly absorbing media. *Nat. Mater.* **2013**, *12*, 20–24.
[95] Yoo, Y. J.; Lim, J. H.; Lee, G. J.; Jang, K. I.; Song, Y. M. Ultra-thin films with highly absorbent porous media fine-tunable for coloration and enhanced color purity. *Nanoscale* **2017**, *9*, 2986–2991.
[96] Yoo, Y. J. Y.; Ko, J. H.; Kim, W. G.; Kim, Y. J.; Kong, D. J.; Kim, S.; Oh, J. W.; Song, Y. M. Dual-mode colorimetric sensor based on ultrathin resonating facilitator capable of nanometer-thick virus detection for environment monitoring. *ACS Appl. Nano Mater.* **2020**, *3*, 6636–6644.
[97] Kim, Y. J.; Yoo, Y. J.; Lee, G. J.; Yoo, D. E.; Lee, D. W.; Siva, V.; Song, H.; Kang, I. S.; Song, Y. M. Enlarged color gamut representation enabled by transferable silicon nanowire arrays on metal–insulator–metal films. *ACS Appl. Mater. Interfaces* **2019**, *11*, 11849–11856.
[98] Yoo, Y. J.; Kim, W. G.; Ko, J. H.; Kim, Y. J.; Lee, Y.; Stanciu, S. G.; Lee, J. M.; Kim, S.; Oh, J. W.; Song, Y. M. Large-area virus coated ultrathin colorimetric sensors with a highly lossy resonant promoter for enhanced chromaticity. *Adv. Sci.* **2020**, *7*, 2000978.
[99] Kou, D. H.; Ma, W.; Zhang, S. F.; Lutkenhaus, J. L.; Tang, B. T. High-performance and multifunctional colorimetric humidity sensors based on mesoporous photonic crystals and nanogels. *ACS Appl. Mater. Interfaces* **2018**, *10*, 41645–41654.
[100] Jung, S. H.; Jung, Y. J.; Park, B. C.; Kong, H.; Lim, B.; Park, J. M.; Lee, H. I. Chromophore-free photonic multilayer films for the ultra-sensitive colorimetric detection of nerve agent mimics in the vapor phase. *Sens. Actuators B Chem.* **2020**, *323*, 128698.
[101] Bai, L.; Wang, Z. L.; He, Y. D.; Song, F.; Wang, X. L.; Wang, Y. Z. Flexible photonic cellulose nanocrystal films as a platform with multisensing functions. *ACS Sustain Chem. Eng.* **2020**, *8*, 18484–18491.
[102] Gallego-Gómez, F.; Morales, M.; Blanco, A.; López, C. Bare silica opals for real-time humidity sensing. *Adv. Mater. Technol.* **2019**, *4*, 1800493.
[103] Kim, S.; Mitropoulos, A. N.; Spitzberg, J. D.; Tao, H.; Kaplan, D. L.; Omenetto, F. G. Silk inverse opals. *Nat. Photonics* **2012**, *6*, 818–823.
[104] Jiang, Y. N.; Zhang, X. J.; Xiao, L. Z.; Yan, R. Y.; Xin, J. W.; Yin, C. X.; Jia, Y. X.; Zhao, Y.; Xiao, C. Y.; Zhang, Z. et al. Preparation of dual-emission polyurethane/carbon dots thermoresponsive composite films for colorimetric temperature sensing. *Carbon* **2020**, *163*, 36–33.
[105] Feng, J. F.; Gao, S. Y.; Shi, J. L.; Liu, T. F.; Cao, R. C-QDs@UIO-66-$(COOH)_2$ composite film via electrophoretic deposition for temperature sensing. *Inorg. Chem.* **2018**, *57*, 2447–2454.
[106] Zhang, L. F.; Lyu, S. Y.; Zhang, Q. J.; Wu, Y. T.; Melcher, C.; Chmely, S. C.; Chen, Z. L.; Wang, S. Q. Dual-emitting film with cellulose nanocrystal-assisted carbon dots grafted $SrAl_2O_4$, Eu^{2+}, Dy^{3+} phosphors for temperature sensing. *Carbohydr. Polym.* **2019**, *206*, 767–777.
[107] Park, T. H.; Yu, S.; Cho, S. H.; Kang, H. S.; Kim, Y.; Kim, M. J.; Eoh, H.; Park, C.; Jeong, B.; Lee, S. W. et al. Block copolymer structural color strain sensor. *NPG Asia Mater.* **2018**, *10*, 328–339.
[108] Kim, D. Y.; Choi, S.; Cho, H.; Sun, J. Y. Electroactive soft photonic devices for the synesthetic perception of color and sound. *Adv. Mater.* **2019**, *31*, 1804080.
[109] Takeoka, Y.; Watanabe, M. Tuning structural color changes of porous thermosensitive gels through quantitative adjustment of the cross-linker in pre-gel solutions. *Langmuir* **2003**, *19*, 9104–9106.
[110] Wang, H.; Zhang, K. Q. Photonic crystal structures with tunable structure color as colorimetric sensors. *Sensors* **2013**, *13*, 4192–4213.
[111] Tu, K. N.; Liu, Y. X.; Li, M. L. Effect of joule heating and current crowding on electromigration in mobile technology. *Appl. Phys. Rev.* **2017**, *4*, 011101.
[112] Zhu, L. X.; Raman, A.; Wang, K. X.; Anoma, M. A.; Fan, S. H. Radiative cooling of solar cells. *Optica* **2014**, *1*, 32–38.
[113] Dou, S. L.; Xu, H. B.; Zhao, J. P.; Zhang, K.; Li, N.; Lin, Y. P.; Pan, L.; Li, Y. Bioinspired microstructured materials for optical and thermal regulation. *Adv. Mater.* **2021**, *33*, 2000697.
[114] Ahn, J.; Lim, T.; Yeo, C. S.; Hong, T.; Jeong, S. M.; Park, S. Y.; Ju, S. Infrared invisibility cloak based on polyurethane–tin oxide composite microtubes. *ACS Appl. Mater. Interfaces* **2019**, *11*, 14296–14304.
[115] Lee, J.; Sul, H.; Jung, Y.; Kim, H.; Han, S.; Choi, J.; Shin, J.; Kim, D.; Jung, J.; Hong, S. et al. Thermally controlled, active imperceptible artificial skin in visible-to-infrared range. *Adv. Funct. Mater.* **2020**, *30*, 2003328.
[116] Lee, N.; Kim, T.; Lim, J. S.; Chang, I.; Cho, H. H. Metamaterial-selective emitter for maximizing infrared camouflage performance with energy dissipation. *ACS Appl. Mater. Interfaces* **2019**, *11*, 21250–21257.
[117] Franklin, D.; Modak, S.; Vázquez-Guardado, A.; Safaei, A.; Chanda, D. Covert infrared image encoding through imprinted plasmonic cavities. *Light Sci Appl* **2018**, *7*, 93.
[118] Lee, G. J.; Kim, D. H.; Heo, S. Y.; Song, Y. M. Spectrally and spatially selective emitters using polymer hybrid spoof plasmonics. *ACS Appl. Mater. Interfaces* **2020**, *12*, 53206–53214.
[119] Qian, Z. Y.; Kang, S.; Rajaram, V.; Cassella, C.; McGruer, N. E.; Rinaldi, M. Zero-power infrared digitizers based on plasmonically enhanced micromechanical photoswitches. *Nat. Nanotechnol.* **2017**, *12*, 969–973.
[120] Hu, R.; Zhou, S. L.; Li, Y.; Lei, D. Y.; Luo, X. B.; Qiu, C. W. Illusion thermotics. *Adv. Mater.* **2018**, *30*, 1707237.
[121] Xie, X.; Li, X.; Pu, M. B.; Ma, X. L.; Liu, K. P.; Guo, Y. H.; Luo, X. G. Plasmonic metasurfaces for simultaneous thermal infrared invisibility and holographic illusion. *Adv. Funct. Mater.* **2018**, *28*, 1706673.
[122] Kim, J.; Han, K.; Hahn, J. W. Selective dual-band metamaterial perfect absorber for infrared stealth technology. *Sci. Rep.* **2017**, *7*, 6740.
[123] Xu, Z. Q.; Li, Q.; Du, K. K.; Long, S. W.; Yang, Y.; Cao, X.; Luo, H.; Zhu, H. Z.; Ghosh, P.; Shen, W. D. et al. Spatially resolved

dynamically reconfigurable multilevel control of thermal emission. *Laser Photonics Rev.* **2020**, *14*, 1900162.
[124] Bakan, G.; Ayas, S.; Serhatlioglu, M.; Elbuken, C.; Dana, A. Invisible thin-film patterns with strong infrared emission as an optical security feature. *Adv. Opt. Mater.* **2018**, *6*, 1800613.
[125] Raman, A. P.; Anoma, M. A.; Zhu, L. X.; Rephaeli, E.; Fan, S. H. Passive radiative cooling below ambient air temperature under direct sunlight. *Nature* **2014**, *515*, 540–544.
[126] Li, T.; Zhai, Y.; He, S. M.; Gan, W. T.; Wei, Z. Y.; Heidarinejad, M.; Dalgo, D.; Mi, R. Y.; Zhao, X. P.; Song, J. W. et al. A radiative cooling structural material. *Science* **2019**, *364*, 760–763.
[127] Hsu, P. C.; Liu, C.; Song, A. Y.; Zhang, Z.; Peng, Y. C.; Xie, J.; Liu, K.; Wu, C. L.; Catrysse, P. B.; Cai, L. L. A dual-mode textile for human body radiative heating and cooling. *Sci. Adv.* **2017**, *3*, e1700895.
[128] Heo, S. Y.; Lee, G. J.; Kim, D. H.; Kim, Y. J.; Ishii, S.; Kim, M. S.; Seok, T. J.; Lee, B. J.; Lee, H.; Song, Y. M. A Janus emitter for passive heat release from enclosures. *Sci. Adv.* **2020**, *6*, eabb1906.
[129] Lee, G. J.; Kim, Y. J.; Kim, H. M.; Yoo, Y. J.; Song, Y. M. Colored, daytime radiative coolers with thin-film resonators for aesthetic purposes. *Adv. Opt. Mater.* **2018**, *6*, 1800707.
[130] Kang, M. H.; Lee, G. J.; Lee, J. H.; Kim, M. S.; Yan, J.; Jeong, J. W.; Jang, K.; Song, Y. M. Outdoor-useable, wireless/battery-free patch-type tissue oximeter with radiative cooling. *Adv. Sci.*, **2021**.
[131] Zhou, Y. P.; Liu, Y. N.; Li, Y.; Jiang, R. M.; Li, W. X.; Zhao, W. C.; Mao, R.; Deng, L. J.; Zhou, P. H. Flexible radiative cooling material based on amorphous alumina nanotubes. *Opt. Mater. Express* **2020**, *10*, 1641–1648.
[132] Mandal, J.; Fu, Y. K.; Overvig, A. C.; Jia, M. X.; Sun, K. R.; Shi, N. N.; Zhou, H.; Xiao, X. H.; Yu, N. F.; Yang, Y. Hierarchically porous polymer coatings for highly efficient passive daytime radiative cooling. *Science* **2018**, *362*, 315–319.
[133] Low, T.; Avouris, P. Graphene plasmonics for terahertz to mid-infrared applications. *ACS Nano* **2014**, *8*, 1086–1101.
[134] Hu, F. J.; Lucyszyn, S. Ultra-low cost ubiquitous THZ security systems. In *Asia-Pacific Microwave Conference 2011*, Melbourne, Australia, 2011, pp 60–62.
[135] Nie, S. M.; Emory, S. R. Probing single molecules and single nanoparticles by surface-enhanced Raman scattering. *Science* **1997**, *275*, 1102–1106.
[136] Tonouchi, M. Cutting-edge terahertz technology. *Nat. Photonics* **2007**, *1*, 97–105.
[137] Ferguson, B.; Zhang, X. C. Materials for terahertz science and technology. *Nat. Mater.* **2002**, *1*, 26–33.
[138] Soref, R. Mid-infrared photonics in silicon and germanium. *Nat. Photonics* **2010**, *4*, 495–497.
[139] Wang, C. Y.; Herr, T.; Del'Haye, P.; Schliesser, A.; Hofer, J.; Holzwarth, R.; Hänsch, T. W.; Picqué, N.; Kippenberg, T. J. Mid-infrared optical frequency combs at 2.5 μm based on crystalline microresonators. *Nat. Commun.* **2013**, *4*, 1345.
[140] Jin, T. N.; Lin, H. Y. G.; Tiwald, T.; Lin, P. T. Flexible mid-infrared photonic circuits for real-time and label-free hydroxyl compound detection. *Sci. Rep.* **2019**, *9*, 4153.
[141] Aksu, S.; Huang, M.; Artar, A.; Yanik, A. A.; Selvarasah, S.; Dokmeci, M. R.; Altug, H. Flexible plasmonics on unconventional and nonplanar substrates. *Adv. Mater.* **2011**, *23*, 4422–4430.
[142] Shen, X. P.; Cui, T. J.; Martin-Cano, D.; Garcia-Vidal, F. J. Conformal surface plasmons propagating on ultrathin and flexible films. *Proc. Natl. Acad. Sci. USA* **2013**, *110*, 40–45.
[143] Lin, P. T.; Jung, H.; Kimerling, L. C.; Agarwal, A.; Tang, H. X. Low-loss aluminium nitride thin film for mid-infrared microphotonics. *Laser Photonics Rev.* **2014**, *8*, L23–L28.
[144] Limaj, O.; Etezadi, D.; Wittenberg, N. J.; Rodrigo, D.; Yoo, D.; Oh, S. H.; Altug, H. Infrared plasmonic biosensor for real-time and label-free monitoring of lipid membranes. *Nano Lett.* **2016**, *16*, 1502–1508.
[145] Chang, C. Y.; Lin, H. T.; Lai, M. S.; Shieh, T. Y.; Peng, C. C.; Shih, M. H.; Tung, Y. C. Flexible localized surface plasmon resonance sensor with metal–insulator–metal nanodisks on PDMS substrate. *Sci. Rep.* **2018**, *8*, 11812.
[146] Kim, S. S.; Young, C.; Mizaikoff, B. Miniaturized mid-infrared sensor technologies. *Anal. Bioanal. Chem.* **2008**, *390*, 231–237.
[147] Salemizadeh, M.; Mahani, F. F.; Mokhtari, A. Tunable mid-infrared graphene-titanium nitride plasmonic absorber for chemical sensing applications. *J. Opt. Soc. Am. B* **2019**, *36*, 2863–2870.
[148] Rowe, D. J.; Smith, D.; Wilkinson, J. S. Complex refractive index spectra of whole blood and aqueous solutions of anticoagulants, analgesics and buffers in the mid-infrared. *Sci. Rep.* **2017**, *7*, 7356.
[149] Asgari, S.; Kashani, Z. G.; Granpayeh, N. Tunable nano-scale graphene-based devices in mid-infrared wavelengths composed of cylindrical resonators. *J. Opt.* **2018**, *20*, 045001.
[150] Xu, K. C.; Wang, Z. Y.; Tan, C. F.; Kang, N.; Chen, L. W.; Ren, L.; Thian, E. S.; Ho, G. W.; Ji, R.; Hong, M. H. Uniaxially stretched flexible surface Plasmon resonance film for versatile surface enhanced Raman scattering diagnostics. *ACS Appl. Mater. Interfaces* **2017**, *9*, 26341–26349.
[151] Yang, X. X.; Zhai, F.; Hu, H.; Hu, D. B.; Liu, R. N.; Zhang, S. P.; Sun, M. T.; Sun, Z. P.; Chen, J. N.; Dai, Q. Far-field spectroscopy and near-field optical imaging of coupled Plasmon–phonon polaritons in 2D van der Waals heterostructures. *Adv. Mater.* **2016**, *28*, 2931–2938.
[152] Hu, H.; Guo, X. D.; Hu, D. B.; Sun, Z. P.; Yang, X. X.; Dai, Q. Flexible and electrically tunable plasmons in graphene–mica heterostructures. *Adv. Sci.* **2018**, *5*, 1800175.
[153] Hänsel, K.; Wilde, N.; Haddadi, H.; Alomainy, A. Challenges with current wearable technology in monitoring health data and providing positive behavioural support. In *Proceedings of the 5th EAI International Conference on Wireless Mobile Communication and Healthcare*, Brussels, Belgium, 2015, pp 158–161.
[154] Herder, C.; Yu, M. D.; Koushanfar, F.; Devadas, S. Physical unclonable functions and applications: A tutorial. *Proc. IEEE* **2014**, *102*, 1126–1141.
[155] Committee on Armed Services, United States Senate. *Inquiry into Counterfeit Electronic Parts in the Department of Defense Supply Chain*; U.S. Government Printing Office: Washington, DC, USA, 2012; 112–167.
[156] U.S. Department of Commerce. *Defense Industrial Base Assessment: Counterfeit Electronics*; Bureau of Industry and Security, Office of Technology Evaluation: Washington, DC, USA, 2010.
[157] Li, H.; Wu, J. The war in the wearable device market: The analysis from economic perspective. In *Pacific Asia Conference on Information Systems, Chengdu, China*, Atlanta, 2014, pp 147.
[158] Gao, Y. S.; Ranasinghe, D. C.; Al-Sarawi, S. F.; Kavehei, O.; Abbott, D. Emerging physical unclonable functions with nanotechnology. *IEEE Access* **2016**, *4*, 61–80.
[159] O'brien, J.; Lehtonen, K. Counterfeit mobile devices-the duck test. In *Proceedings of 2015 10th International Conference on Malicious and Unwanted Software*, Fajardo, USA, 2015, pp 144–151.
[160] Leem, J. W.; Kim, M. S.; Choi, S. H.; Kim, S. R.; Kim, S. W.; Song, Y. M.; Young, R. J.; Kim, Y. L. Edible unclonable functions. *Nat. Commun.* **2020**, *11*, 328.
[161] Pecht, M.; Tiku, S. Bogus: Electronic manufacturing and consumers confront a rising tide of counterfeit electronics. *IEEE Spectr.* **2006**, *43*, 37–46.
[162] Arppe, R.; Sørensen, T. J. Physical unclonable functions generated through chemical methods for anti-counterfeiting. *Nat. Rev. Chem.* **2017**, *1*, 0031.
[163] Won, P.; Kim, K. K.; Kim, H.; Park, J. J.; Ha, I.; Shin, J.; Jung, J.; Cho, H.; Kwon, J.; Lee, H. et al. Transparent soft actuators/sensors and camouflage skins for imperceptible soft robotics. *Adv. Mater.*, in press, https://doi.org/10.1002/adma.202002397.
[164] Qu, Y. R.; Li, Q.; Cai, L.; Pan, M. Y.; Ghosh, P.; Du, K. K.; Qiu, M. Thermal camouflage based on the phase-changing material GST. *Light Sci. Appl.* **2018**, *7*, 26.
[165] Peng, L.; Liu, D. Q.; Cheng, H. F.; Zhou, S.; Zu, M. A multilayer film based selective thermal emitter for infrared stealth technology. *Adv. Opt. Mater.* **2018**, *6*, 1801006.
[166] Danaeifar, M.; Granpayeh, N. Wideband invisibility by using inhomogeneous metasurfaces of graphene nanodisks in the infrared regime. *J. Opt. Soc. Am. B* **2016**, *33*, 1764–1768.
[167] Zhang, C. L.; Wu, X. Y.; Huang, C.; Peng, J. Q.; Ji, C.; Yang, J. N.; Huang, Y. J.; Guo, Y. H.; Luo, X. G. Flexible and transparent microwave–infrared bistealth structure. *Adv. Mater. Technol.* **2019**, *4*, 1900063.

[168] Morin, S. A.; Shepherd, R. F.; Kwok, S. W.; Stokes, A. A.; Nemiroski, A.; Whitesides, G. M. Camouflage and display for soft machines. *Science* **2012**, *337*, 828–832.
[169] Li, P. N.; Yang, X. S.; Maß, T. W. W.; Hanss, J.; Lewin, M.; Michel, A. K. U.; Wuttig, M.; Taubner, T. Reversible optical switching of highly confined phonon–polaritons with an ultrathin phase-change material. *Nat. Mater.* **2016**, *15*, 870–875.
[170] Collier, R. *Optical Holography*; Elsevier: Amsterdam, 2013.
[171] Picart, P. *New Techniques in Digital Holography*; John Wiley & Sons: London, 2015.
[172] Bianco, V.; Paturzo, M.; Finizio, A.; Ferraro, P. Off-axis self-reference digital holography in the visible and far-infrared region. *ETRI J.* **2019**, *41*, 84–92.
[173] Vandenrijt, J. F.; Thizy, C.; Martin, L.; Beaumont, F.; Garcia, J.; Fabron, C.; Prieto, É.; Maciaszek, T.; Georges, M. P. Digital holographic interferometry in the long-wave infrared and temporal phase unwrapping for measuring large deformations and rigid body motions of segmented space detector in cryogenic test. *Opt. Eng.* **2016**, *55*, 121723.
[174] Georges, M. P.; Thizy, C.; Languy, F.; Vandenrijt, J. F. An overview of interferometric metrology and ndt techniques and applications for the aerospace industry. In *Proceedings of SPIE 9960 Interferometry XVIII*, San Diego, USA, 2016, pp 996007.
[175] Vandenrijt, J. F.; Thizy, C.; Georges, M. P.; Queeckers, P.; Dubois, F.; Doyle, D. Long-wave infrared digital holography for the qualification of large space reflectors. In *Proceedings of SPIE 10564, International Conference on Space Optics—ICSO 2012*, Ajaccio, France, 2017, p 1056403.
[176] Georges, M.; Vandenrijt, J. F.; Thizy, C.; Dubois, F.; Queeckers, P.; Doyle, D.; Pedrini, G.; Alexeenko, I.; Osten, W. Digital holographic interferometry and ESPI at long infrared wavelengths with CO_2 lasers. In *Digital Holography and Three-Dimensional Imaging*, Miami, USA, 2012, pp DW4C.1.
[177] Stoykova, E.; Yaraş, F.; Kang, H.; Onural, L.; Geltrude, A.; Locatelli, M.; Paturzo, M.; Pelagotti, A.; Meucci, R.; Ferraro, P. Visible reconstruction by a circular holographic display from digital holograms recorded under infrared illumination. *Opt. Lett.* **2012**, *37*, 3120–3122.
[178] Paturzo, M.; Pelagotti, A.; Geltrude, A.; Locatelli, M.; Poggi, P.; Meucci, R.; Ferraro, P.; Stoykova, E.; Yaraş, F.; Yontem, A. Ö. et al. Infrared digital holography applications for virtual museums and diagnostics of cultural heritage. In *Proceedings of SPIE 8084, O3A: Optics for Arts, Architecture, and Archaeology III*, Munich, Germany, 2011, p 80840K.
[179] Locatelli, M.; Pugliese, E.; Paturzo, M.; Bianco, V.; Finizio, A.; Pelagotti, A.; Poggi, P.; Miccio, L.; Meucci, R.; Ferraro, P. Imaging live humans through smoke and flames using far-infrared digital holography. *Opt. Express* **2013**, *21*, 5379–5390.
[180] Sun, J. Y.; Hu, F. J.; Lucyszyn, S. Predicting atmospheric attenuation under pristine conditions between 0.1 and 100 THz. *IEEE Access* **2016**, *4*, 9377–9399.
[181] Larouche, S.; Tsai, Y. J.; Tyler, T.; Jokerst, N. M.; Smith, D. R. Infrared metamaterial phase holograms. *Nat. Mater.* **2012**, *11*, 450–454.
[182] Yakhkind, A. K. Optical graded-index elements made from glass. *J. Opt. Technol.* **2003**, *70*, 877–881.
[183] Jin, Y.; Tai, H.; Hiltner, A.; Baer, E.; Shirk, J. S. New class of bioinspired lenses with a gradient refractive index. *J. Appl. Polym. Sci.* **2007**, *103*, 1834–1841.
[184] Freese, W.; Kämpfe, T.; Kley, E. B.; Tünnermann, A. Design of binary subwavelength multiphase level computer generated holograms. *Opt. Lett.* **2010**, *35*, 676–678.
[185] Liu, X. L.; Starr, T.; Starr, A. F.; Padilla, W. J. Infrared spatial and frequency selective metamaterial with near-unity absorbance. *Phys. Rev. Lett.* **2010**, *104*, 207403.
[186] Zhang, S.; Fan, W. J.; Panoiu, N. C.; Malloy, K. J.; Osgood, R. M.; Brueck, S. R. J. Experimental demonstration of near-infrared negative-index metamaterials. *Phys. Rev. Lett.* **2005**, *95*, 137404.
[187] Shalaev, V. M. Optical negative-index metamaterials. *Nat. Photonics* **2007**, *1*, 41–48.
[188] Huang, L. L.; Zhang, S.; Zentgraf, T. Metasurface holography: From fundamentals to applications. *Nanophotonics* **2018**, *7*, 1169–1190.